

We are committed to providing [accessible customer service](#).

If you need accessible formats or communications supports, please [contact us](#).

Nous tenons à améliorer [l'accessibilité des services à la clientèle](#).

Si vous avez besoin de formats accessibles ou d'aide à la communication, veuillez [nous contacter](#).

Report on VTEM Airborne Geophysics at the H-K Project, Ontario

Ranoke Property,
Hecla and Kilmer Townships,
Porcupine Mining Division,
Northeast Region, Ontario
Map Sheet: 42I05

Author:
Justin J. Daley, MSc, PGeo
Principal Geologist
VR Resources Ltd.

October 2020

VR RESOURCES LTD.
2300 – 1177 West Hastings St.
Vancouver, BC, Canada, V6C1G8
Web: www.vrr.ca



Table of Contents

Summary	3
Location and Access	4
Regional Geology and Exploration History	4
Property Exploration History	6
Property Geology	8
Exploration Model	9
Certificate	11
References	12

List of Figures & Tables

Figure 1: Location and access to the Ranoke Property	3
Figure 2: Regional geology map of Kapuskasing structural zone (KSZ)	5
Table 1: Summary of major geological/tectonic events shaping the study region.	6
Figure 3: Panned gold tail from 1970 core recovered by Gary Peacock	7
Figure 4: OGS magnetic data reprocessed for Analytic Signal	8
Figure 5: Schematic section of the exploration target at H-K.	10

Appendix A

Geotech VTEM Report: GL200086

Appendix B

Expense Report

Summary

During the period of June 30th to July 6th, 2020 Geotech Ltd. carried out a helicopter-borne geophysical survey over the Hecla-Kilmer property, located near Otter Rapids, Ontario. The work was performed VR Resources Ltd. of Vancouver, BC in order to help map conductive features in the basement geology in search of Iron-oxide Copper-Gold mineralization within the Hecla-Kilmer Alkali Complex and carbonatite. The flown area is in the Hecla and Kilmer Townships, Porcupine Mining Division, Northeast Region, Ontario. Map sheet 42I05

Principal geophysical sensors included a versatile time domain electromagnetic (VTEMTMPlus) system. Ancillary equipment included a GPS navigation system and a radar altimeter. A total of 459 line-kilometres of geophysical data were acquired during the survey.

In-field data quality assurance and preliminary processing were carried out on a daily basis during the acquisition phase. Preliminary and final data processing, including generation of final digital data and map products were undertaken from the office of Geotech Ltd. in Aurora, Ontario.

****All maps, figures and coordinates are in UTM WGS84 Zone 17****

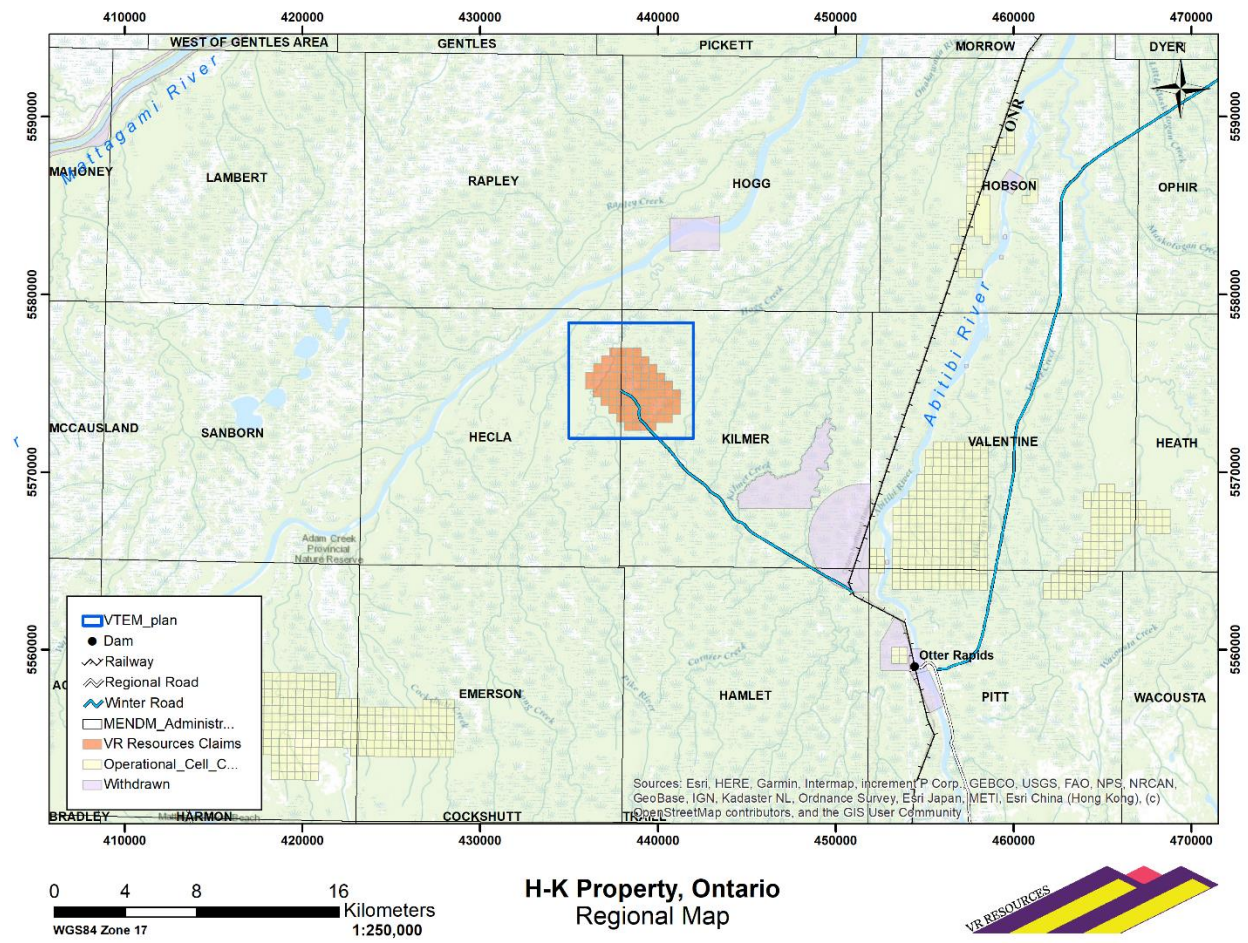


Figure 1: Location and access to the H-K Property

Location and Access

The H-K property is in the Moose River basin in northern Ontario, Canada. It is located south of the Mattagami river. The nearest town is Kapuskasing located on the Trans-Canada Highway (Provincial HWY 11) some 110 kilometres to the southwest. Cochrane is the regional services hub and is located 150 kilometres to the southeast. The property is 15 kilometers west of the active ONR railway line which connects the town of Moosonee with Cochrane on the Trans Canada Highway, thus providing port access to the James Bay region (Figure 1).

Otter Rapids Dam is an Ontario hydroelectric facility located on the Abitibi River about 50 kilometres to the south of the property. Provincial Highway 634 provides road access to Otter Rapids from Smooth Rock Falls, located at the junction of HWY 634 with the Trans-Canada Highway. Private ground just behind the ONR bunk house was rented from Villeneuve Construction and served as camp and helicopter base for crews during drilling. Helicopter access to the property from camp is about 50km each way

The H-K property is located in a boreal region of lowland muskeg, with black spruce and pine forest along river drainages. Topographic relief is minimal, and there is no outcrop in the lowland region; H-K is tens of kilometres north of the northern limit of exposed Archean Superior Province shield in northern Ontario.

Regional Geology and Exploration History

Both the Ranoke and Hecla-Kilmer properties are centered on large magnetic anomalies associated with regional gravity features which occur along the western margin of the Kapuskasing Structural Zone (Figure 2), a long-lived, crustal-scale fault zone which bisects the Archean Superior craton between James Bay and Lake Superior, and hosts numerous alkaline, ultrabasic and carbonatite intrusions and kimberlites which span more than 1.6 billion years of activity. This tectonic setting is prospective for the development of large IOCG or carbonatite-hosted copper-gold hydrothermal breccia systems.

Hecla-Kilmer is a large, roughly circular and concentrically zoned polyphase alkaline intrusive complex with carbonatite approximately 4 – 6 km's across. The complex was emplaced along the regional-scale tectonic suture between two sub-provinces of the Archean Superior Craton; the volcanic-dominated Wabigoon province to the north, and the sediment-dominated Quetico province to the south. Research published by the Ontario Geological Survey in 1988 and based on the petrography and geochemistry of pieces of core obtained from the historic drilling in 1970 described below described the core of the H-K complex as mostly nepheline syenite and phonolite, surrounded by a myriad of ultra-basic and carbonatite intrusive phases including olivine essexite, ijolite, pyroxenite and sovite.

Six diamond drill holes were completed at H-K by Ashland Oil and Elgin Petroleum in 1970 as part of a regional base metal exploration program of the Paleozoic shelf carbonate succession which covers Archean basement rocks in the region. One hole was abandoned, and only 854 m were completed in total in 5 holes, all on magnetic highs in the outer zones of the H-K complex.

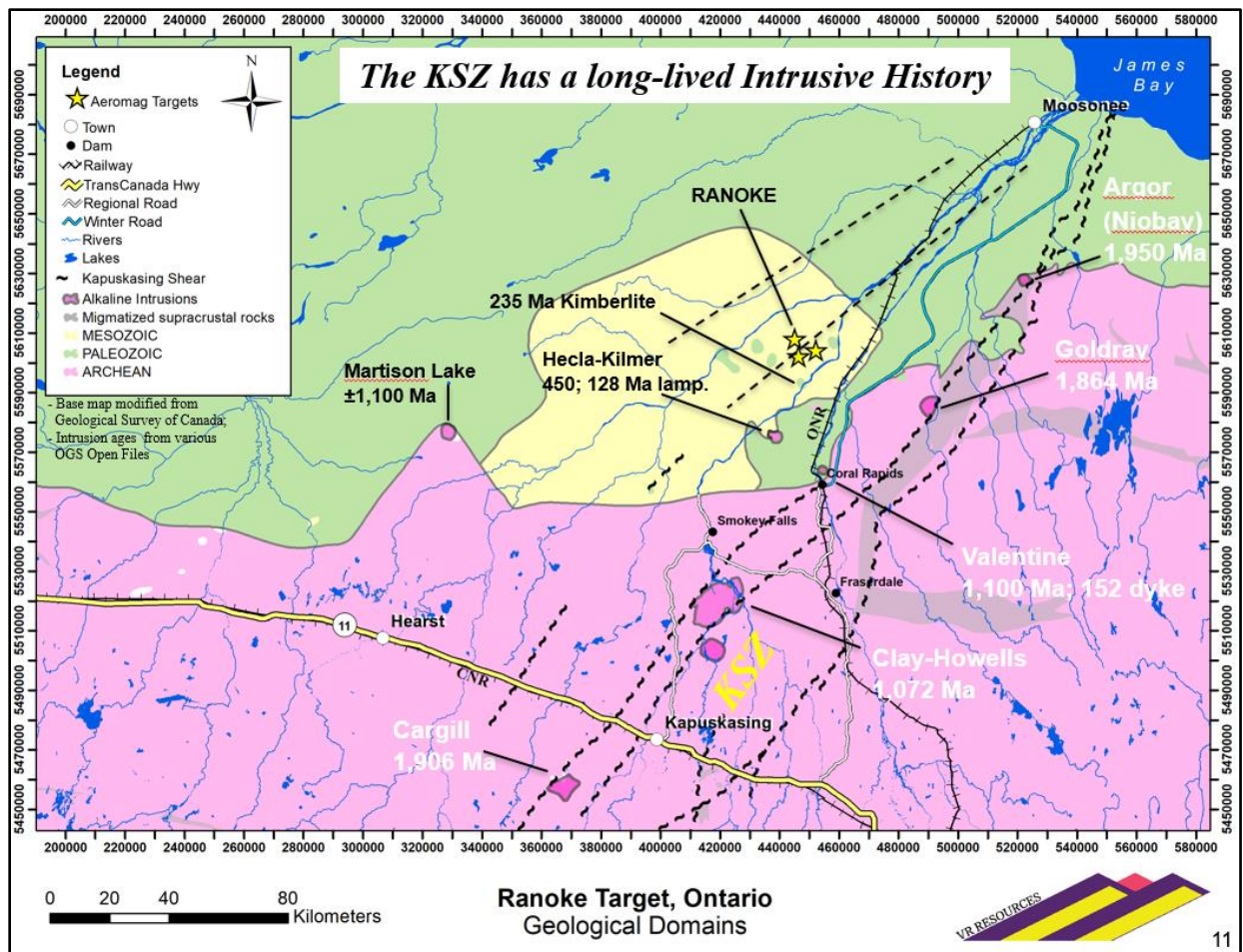


Figure 2: Regional geology map of Kapuskasing structural zone (KSZ) and James Bay Lowlands with alkaline and ultrabasic intrusions and their ages highlighted. The H-K target is noted by 3 gold stars indicating magnetic targets.

Importantly, the historic drilling for base metals in 1970 proved that the H-K carbonatite complex comes to surface, to the base of glacial till and overburden.

Ten years later in 1981, Selco Exploration Company completed two drill holes on peripheral magnetic highs of the complex as part of a regional diamond exploration program, and intersected ultra-basic rocks and mafic breccia.

A high-resolution airborne magnetic survey was flown in the region in 1993 for diamond exploration. The survey shows clearly that Hecla-Kilmer is a concentrically zoned, high contrast magnetic anomaly 4 – 6 km's across. Magnetic boundaries within the complex are sharply defined on RTP, 1VD and 2VD magnetic products. The historic drilling at H-K was done before this high-resolution survey, and before the discovery of the Olympic Dam copper-gold deposit in Australia and the development of the IOCG mineral deposit model, which helps explain why all five holes in 1970 were located in the outer concentric zones of the complex, and why copper-gold-fluorite hydrothermal breccia intersected in drill core in at least one of the holes was not sampled or followed up.

There has been no modern, systematic exploration or drilling of the core of the Hecla-Kilmer intrusive complex for copper and gold in the basement. The opportunity for VR is to be the first to apply modern IOCG and carbonatite mineral deposit models and the first to use modern exploration technologies to explore the core of the H-K complex for a magnetite-copper-gold-fluorite hydrothermal breccia system.

Table 2: Summary of major geological/tectonic events shaping the study region. (Darbyshire et al., 2017)

Date	Event
3–2.6 Ga	Assembly of Superior Craton
2.8–2.6 Ga	Kenoran Orogen completes assembly process
2.49–2.45 Ga	Hotspot influence and rifting on SE Superior margin leads to emplacement of Matachewan dyke swarm
2.2 Ga	Age of Southern Province; Nipissing Sills fed by distant Ungava plume
1.9–1.6 Ga	Penokean Orogen on southern margin of Superior Province; likely age of major uplift in Kapuskasing Structural Zone
~1.8 Ga	Trans-Hudson Orogen on northwest Superior margin
~1.1 Ga	Keweenawan Mid-Continent Rift on southern Superior margin
1.1–1.0 Ga	Grenville Orogen on southeast Superior margin
Late Proterozoic - Early Cambrian	Opening of Ottawa-Bonnechere Graben and Lake Timiskaming structural zone (Ontario/Quebec border region)
Phanerozoic	Development of Hudson Bay and Moose River intracratonic basins
180–134 Ma	Emplacement of kimberlites along track of Great Meteor hotspot

Property Exploration History

The H-K target was previously explored briefly in 1969-1971 when the large alkali complex was mapped by regional magnetics and has a surface area of some 20 km². Historical ground geophysics completed in 1969 shows strong magnetic domains, large structural corridors and identifies eight weak to strong Crone VEM conductors based on sparse cut lines in the central part of the complex. Several conductors extend for up to 400m.

Six diamond drill holes were completed by Ashland Oil and Elgin Petroleum in 1970 as part of a regional base metal exploration program of the Paleozoic shelf carbonate succession which covers Archean basement rocks in the region. One hole was abandoned, and only 854 m were completed in total in 5 holes, all on magnetic highs in the outer zones of the H-K complex. Ten years later in 1981, Selco Exploration Company completed two drill holes on peripheral magnetic highs of the complex as part of a regional diamond exploration program, and intersected ultra-basic rocks and mafic breccia.

The Hecla-Kilmer Alkalic rock complex first documented in OGS Study 38, by Ron P. Sage in 1988. Sage visited an old drill camp and located partially rotted core boxes from 5 wide spaced historical drill holes in summer 1987. The property has no outcrop and is covered by till and

swamp of the James Bay lowlands. Sage collected a suite of rocks from old core samples, and subsequent petrology provided an initial lithology list from five isolated AX core holes.

A high-resolution airborne magnetic survey was flown in the region in 1993 for diamond exploration. The survey shows clearly that Hecla-Kilmer is a concentrically zoned, high contrast magnetic anomaly 4 – 6 km's across. Magnetic boundaries within the complex are sharply defined on RTP, 1VD and 2VD magnetic products. The historic drilling at H-K was done before this high-resolution survey, and before the discovery of the Olympic Dam copper-gold deposit in Australia and the development of the IOCG mineral deposit model, which helps explain why all five holes in 1971 were located in the outer concentric zones of the complex, and why copper-gold-fluorite hydrothermal breccia intersected in drill core in at least one of the holes was not sampled or followed up.

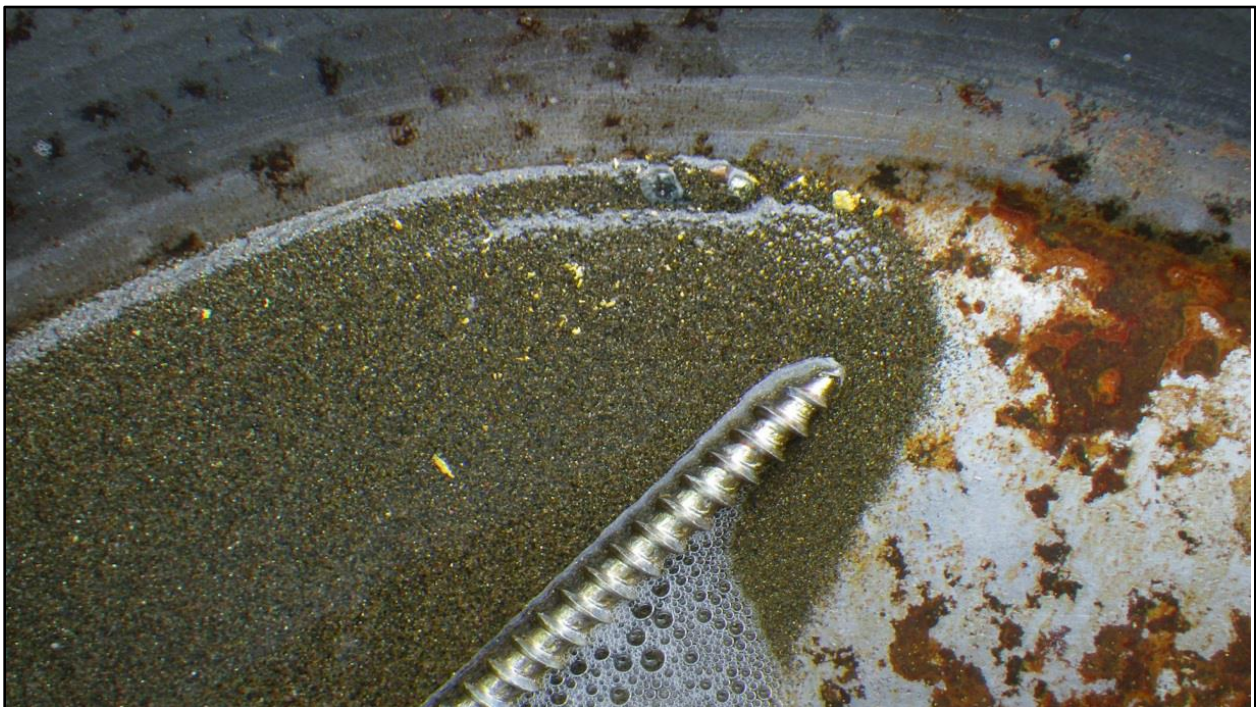


Figure 3: Gold tail from Batch 1 of H-K core recovery clean up by Gary Peacock

Gary Peacock and later Orebot Inc. staked the Alkalic Complex in 2012 and 2015 in search of diamond bearing kimberlite in addition to I-510, a historical BP-Selco diamond-bearing melilitite discovery that is part of the Coral Rapids cluster. Historical drill logs mention a lamprophyre and also describe some of the breccias as kimberlite at Pike River. This encouraged Gary to also find the old drill camp and sample old drill core previously sampled by Sage, 1988. The 45-year old core was grown over by moss and deeply weathered. Gary Peacock, an expert mineral processor devised a way to clean the core by tumbling it in a cement mixer with sand and water in a heavy mineral lab he built at his residence. After many hours of tumbling, each piece of core was clean and primary rock textures were once again visible. Core was removed from the cement mixer and placed in drill core boxes in random order. Gary panned the sandy residue in bottom of the cement mixer and discovered gold, not trace amounts, but a significant gold tail with +1mm nuggets.

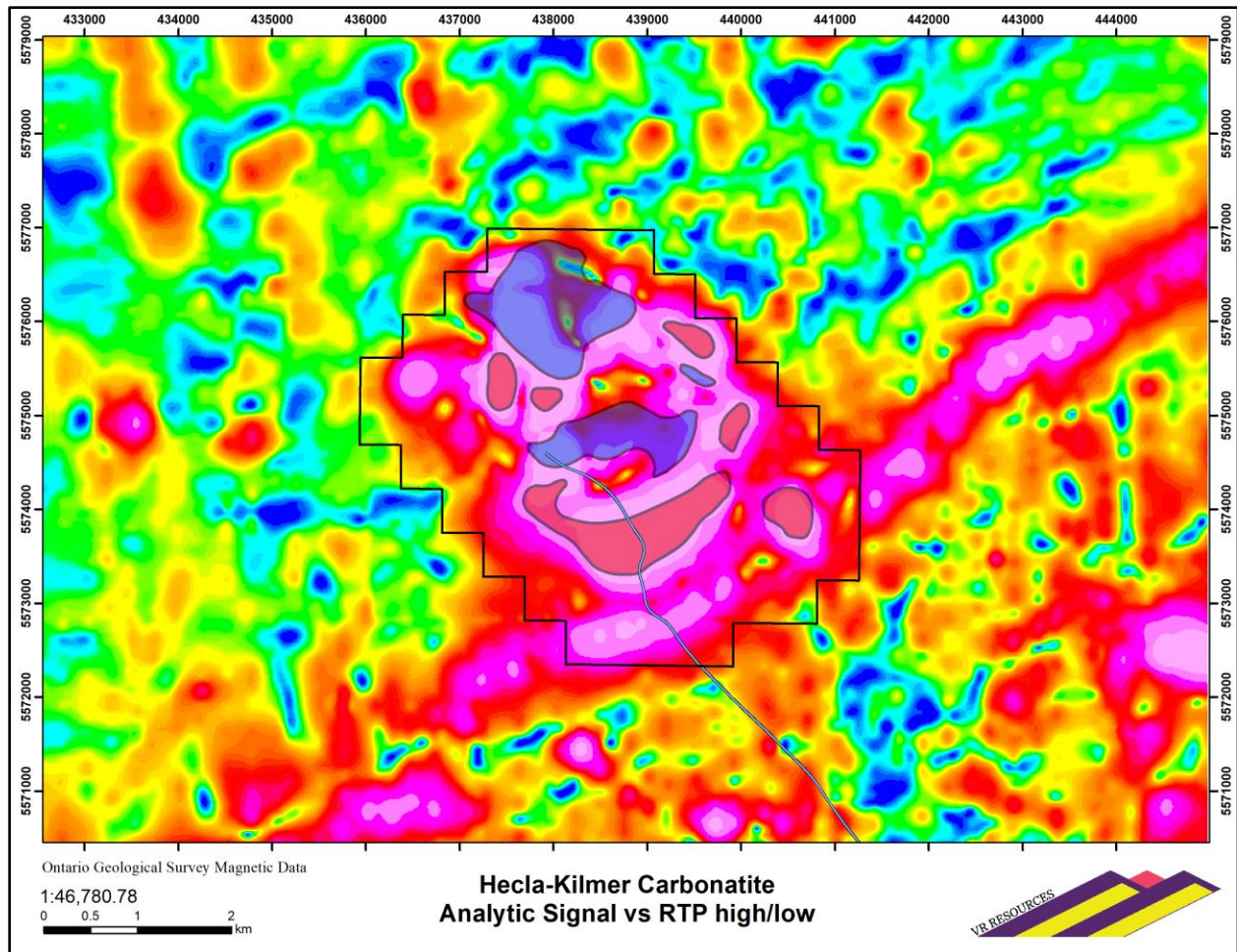


Figure 4: Magnetic Analytic Signal at H-K from the 1993 Highsense survey and regional OGS magnetic data showing staking over the high contrast magnetic complex of the Hecla-Kilmer Alkali Complex. The complex occurs at the suture of the Wabigoon and Quetico Subprovinces of the Superior Craton and structurally controlled by the intersection of Archean Mattachewan (NNE-SSW) and Biscotasing (SW-NE) dyke swarms. RTP anomalies are shaded in red and blue outlines and are relatively discordant with analytic signal, which may indicate hydrothermal magnetite.

Property Geology

Till overburden at the H-K Property is roughly 50-100m thick and sits above a glacially eroded Archean basement that is locally and unconformably overlain by the Upper Silurian Sextant Formation, comprising deep red limonitic sandstones at the weathered erosional contact and grades upward into a coarse reduced arenite and chemically-deposited limestone, primary dolomite and thin muddy breccia.

Hecla-Kilmer is a large, polyphase Proterozoic alkaline intrusive complex with carbonatite approximately 4 – 6 km's across. The core of the complex is mostly nepheline syenite and phonolite, surrounded by a myriad of ultra-basic and carbonatite intrusive phases including soviet, ijolite, pyroxenite and olivine gabbro. The complex was emplaced along the regional-

scale tectonic suture between two sub-provinces of the Archean Superior Craton; the volcanic-dominated Wabigoon province to the north, and the sediment-dominated Quetico province to the south. Evident in magnetic surveys and drilling regionally are regularly spaced and continuous mafic Matachewan and Biscotasing dykes emplaced in the Archean. These dykes are perpendicular relative to each other and form the basis of regional structural movement and are the focus of hydrothermal-magmatic fluids and related intrusions.

Basement units are cross-cut by much later aphanitic lamprophyre plugs and dykes that are ferroan and alkalic in nature and often contain calcite amygdaloids and phlogopite lathes (Figure 5, Photo 1). These late dykes often have brittle intrusive contacts with angular wall rock clasts and are rarely more than 1.5 m across. The brittle nature and movement indicators on the contacts indicates the lamprophyres have intruded along active faults.

Exploration Model

H-K is located immediately north of a robust copper-gold-fluorite heavy mineral anomaly evident in several rivers in the Coral Rapids area, based on a regional alluvium survey completed by the Ontario Geological Survey in 2001 and 2002. The unique mineral assemblage underscores the potential for a buried carbonatite or IOCG deposit (iron oxide copper-gold) as the source of the geochemical anomaly.

The H-K property covers a well defined, high intensity magnetic complex approximately 5 x 5 kilometres in size and evident on regional-scale Geological Survey of Canada (GSC) aeromagnetic maps. The complex delineates a regional-scale structural suture zones and structural intersections of Archean dykes, and individual magnetic anomalies are locally discordant to the regional magnetic grain evident in Archean basement rocks. The high resolution airborne survey completed by High Sense in 1993 confirmed the location, geometry and intensity of the H-K complex evident on the historic GSC maps. The northern magnetic anomaly at H-K is both the largest, at > 500m's in diameter, and the highest intensity, at > 1,000 nT. It has a vertical, pipe-like geometry with sharply defined margins and a central apex which is consistent across TMI, RTP and 1VD magnetic products.

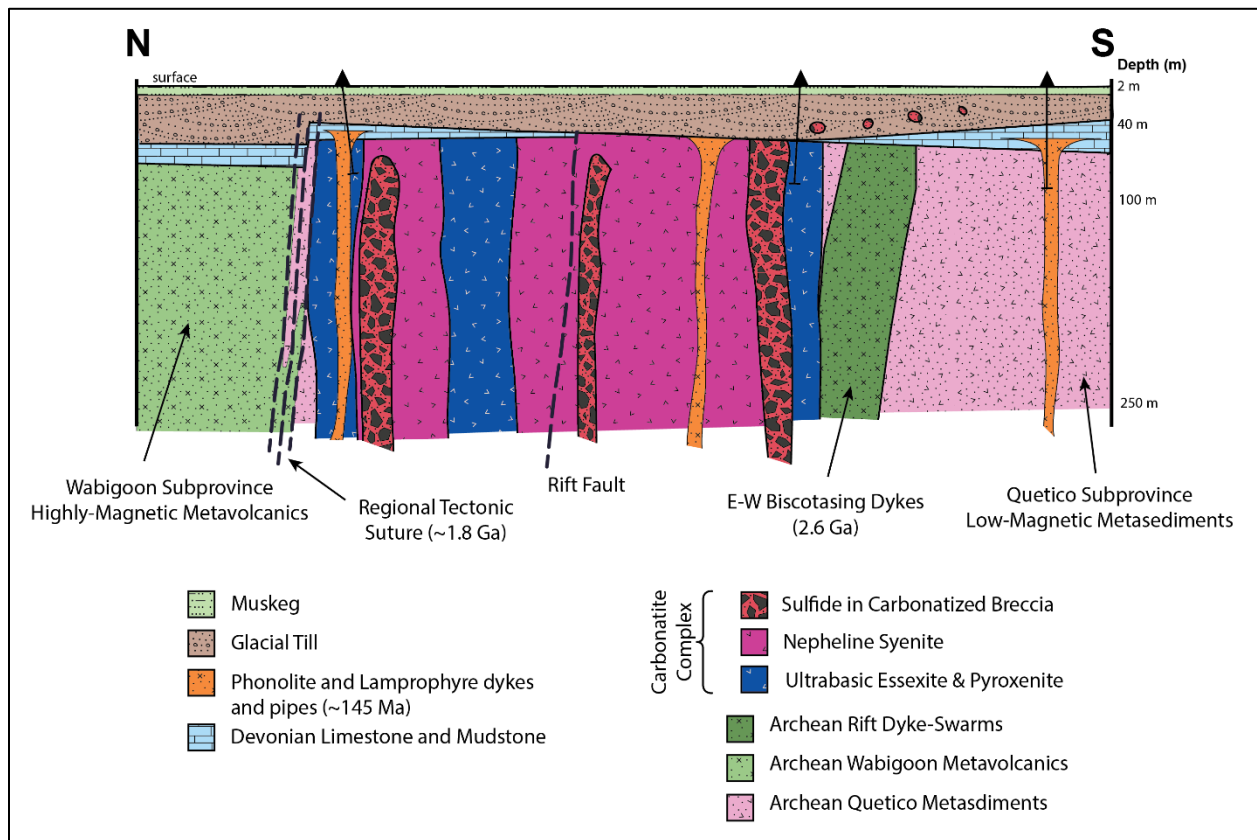


Figure 5: Schematic section of the exploration target at H-K.

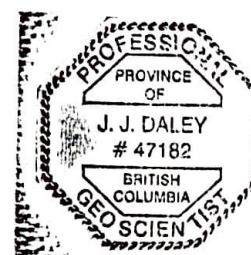
The schematic cross-section shown in Figure 6 illustrates the target at H-K; a near-surface, large, vertical, magnetic, dense IOCG pipe or carbonatite intrusion. This cross-section is a representation of the discreet magnetic anomaly (pipe) at the northern end of the overall magnetic complex and structural intersection at H-K. This pipe is potentially the near-surface but till-covered source to copper and gold grains observed in the unconsolidated overburden in nearby reverse circulation drill holes completed in the early 1980's during a reconnaissance evaluation of Cretaceous-aged coal seams in the Moose River Basin.

Certificate

1. I, Justin J. Daley, reside at 451 Kingswood Rd., Toronto, Ontario, M4E3P4
2. I have a B.Sc. Honours in Geological Sciences from Queen's University in Kingston, ON (2012) and a M.Sc. in Geology (Mineral Exploration) from Laurentian University in Sudbury, ON (2017).
3. I am a registered Professional Geoscientist in the Province of British Columbia and have been for three years.
4. I have been involved in all aspects of mineral exploration for 10 years in the United States, Mexico, Chile, Peru, and across Canada in British Columbia, Saskatchewan, Yukon Territory and Ontario.
5. I have primarily worked within magmatic-hydrothermal systems, such as Cu-Mo-Au porphyries, Au-Ag epithermal deposits and iron-oxide copper gold deposits, for the last 10 years.
6. I am not aware of any material fact or of any material change with respect to the subject matter of this technical report, which has not been reviewed and might make the report misleading.
7. I am a non-independent person with respect to VR Resources, I own shares and have received option agreements with respect to my work with the company as "Principal Geologist" from 2017 to present.

Dated at Toronto, Ontario on Sept. 29, 2020


Justin J. Daley, PGeo



References

Darbyshire, F. A., Eaton, D. W., Frederiksen, A. W., & Ertolahti, L. 2007. New insights into the lithosphere beneath the Superior Province from Rayleigh wave dispersion and receiver function analysis. *Geophysical Journal International*, 169(3), 1043-1068.

Halls, H. C., & Davis, D. W., 2004. Paleomagnetism and U Pb geochronology of the 2.17 Ga Biscotasing dyke swarm, Ontario, Canada: evidence for vertical-axis crustal rotation across the Kapuskasing Zone. *Canadian Journal of Earth Sciences*, 41(3), 255-269.

Sage, R. P., 1988. Geology of Carbonatite – Alkalic Rock Complexes in Ontario: Hecla-Kilmer Alkalic Rock Complex. District of Cochrane. Ontario Geological Survey Study 38. ISSN 0704-2590; 38p

Salo, R. W., 2006. Diamond Drilling Report On The Coral Rapids Property For Baltic Resources Inc., OGS Assessment Report Database. Assessment File: 20000001302. AFRO Number: 2.31852. Resident Geologist District: Timmins. Resident Geologist Office File Number: T-5357

Winchester, J.A. and Floyd, P.A., 1977. Geochemical discrimination of different magma series and their differentiation products using immobile elements. *Chemical geology*, 20, pp.325-343.



VTEM™ Plus

REPORT ON A HELICOPTER-BORNE VERSATILE TIME DOMAIN
ELECTROMAGNETIC (VTEM™ Plus) GEOPHYSICAL SURVEY

PROJECT: HECLA-KILMER PROPERTY
LOCATION: OTTER RAPIDS, ONTARIO
FOR: VR RESOURCES LIMITED
SURVEY FLOWN: JUNE - JULY 2020
PROJECT: GL200086

Geotech Ltd.
270 Industrial Parkway South
Aurora, ON Canada L4G 3T9

Tel: +1 905 841 5004
Web: www.geotech.ca
Email: info@geotech.ca



TABLE OF CONTENTS

EXECUTIVE SUMMARY	3
1. INTRODUCTION	4
1.1 General Considerations	4
1.2 Survey and System Specifications	5
1.3 Topographic Relief and Cultural Features	6
2. DATA ACQUISITION	7
2.1 Survey Area	7
2.2 Survey Operations	7
2.3 Flight Specifications	7
2.4 Aircraft and Equipment	8
2.4.1 Survey Aircraft.....	8
2.4.2 Electromagnetic System	8
2.4.3 Full waveform vtem™ sensor calibration.....	12
2.4.4 Radar Altimeter.....	12
2.4.5 GPS Navigation System	12
2.4.6 Digital Acquisition System.....	12
3. PERSONNEL	13
4. DATA PROCESSING AND PRESENTATION	14
4.1 Flight Path.....	14
4.2 Electromagnetic Data.....	14
5. DELIVERABLES	16
5.1 Survey Report	16
5.2 Maps.....	16
5.3 Digital Data	17
5.3.1 DVD Structure	17
5.3.2 Database of the Apparent Resistivity Depth Imaging Products	19
5.3.3 Database of the VTEM Waveform.....	19
5.3.4 Resistivity Depth Image Products.....	19
5.3.5 Grids in Geosoft GRD and GeoTIFF format.....	20
6. CONCLUSIONS AND RECOMMENDATIONS	21

LIST OF FIGURES

Figure 1: Survey location	4
Figure 2: Survey area location on Google Earth.....	5
Figure 3: Flight path over a Google Earth Image.	6
Figure 4: VTEM™plus Transmitter Current Waveform	8
Figure 5: VTEM™plus System Configuration.....	11
Figure 7: Z, X and Fraser filtered X (FFx) components for “thin” target.....	15

LIST OF TABLES

Table 1: Survey Specifications.....	7
Table 2: Survey schedule	7
Table 3: Off-Time Decay Sampling Scheme	9
Table 4: Acquisition Sampling Rates.....	12
Table 5: Geosoft GDB Data Format	17
Table 6: Geosoft Apparent Resistivity Depth Image GDB Data Format.....	19
Table 7: Geosoft database for the VTEM waveform	19

APPENDICES

A.	Survey Location Maps
B.	Survey Survey Area Coordinates
C.	Geophysical Maps
D.	Generalized Modelling Results of the VTEM System.....
E.	TAU Analysis
F.	TEM Resistivity Depth Imaging (RDI).....
G.	Resistivity Depth Images (RDI).....

EXECUTIVE SUMMARY

HECLA-KILMER PROPERTY OTTER RAPIDS, ONTARIO

During the period of June 30th to July 6th, 2020 Geotech Ltd. carried out a helicopter-borne geophysical survey over the Hecla-Kilmer property, located near Otter Rapids, Ontario.

Principal geophysical sensors included a versatile time domain electromagnetic (VTEM™Plus) system. Ancillary equipment included a GPS navigation system and a radar altimeter. A total of 459 line-kilometres of geophysical data were acquired during the survey.

In-field data quality assurance and preliminary processing were carried out on a daily basis during the acquisition phase. Preliminary and final data processing, including generation of final digital data and map products were undertaken from the office of Geotech Ltd. in Aurora, Ontario.

The processed survey results are presented as the following maps:

- Electromagnetic stacked profiles of the B-field Z Component
- Electromagnetic stacked profiles of dB/dt Z Components
- B-Field Z Component Channel grids for early, middle and late time
- Fraser Filtered X Component Channel grid
- Calculated Time Constant (Tau)
- Resistivity Depth Image (RDI) sections and slices

Digital data includes all electromagnetic products, plus ancillary data including the waveform.

The survey report describes the procedures for data acquisition, equipment used, processing, final image presentation and the specifications for the digital data set.

1. INTRODUCTION

1.1 GENERAL CONSIDERATIONS

Geotech Ltd. performed a helicopter-borne geophysical survey over the Hecla-Kilmer property, located approximately 20 km northwest of Otter Rapids, Ontario (Figure 1 & Figure 2).

Michael Gunning and Justin Daley represented VR Resources Limited during the data acquisition and data processing phases of this project.

The geophysical surveys consisted of helicopter borne EM using the versatile time-domain electromagnetic (VTEM) Plus system with Full-Waveform processing. Measurements consisted of vertical (Z), in-line and cross-line horizontal (X & Y), components of the EM field using induction coils. A total of 459 line-km of geophysical data were acquired during the survey.

The crew was based out of Kapuskasing (Figure 2) in Ontario for the acquisition phase of the survey. Survey flying started June 30th and was completed on July 6th, 2020.

Data quality control and quality assurance, and preliminary data processing were carried out on a daily basis during the acquisition phase of the project. Final data processing followed immediately after the end of the survey. Final reporting, data presentation and archiving were completed from the Aurora office of Geotech Ltd. in August 2020.

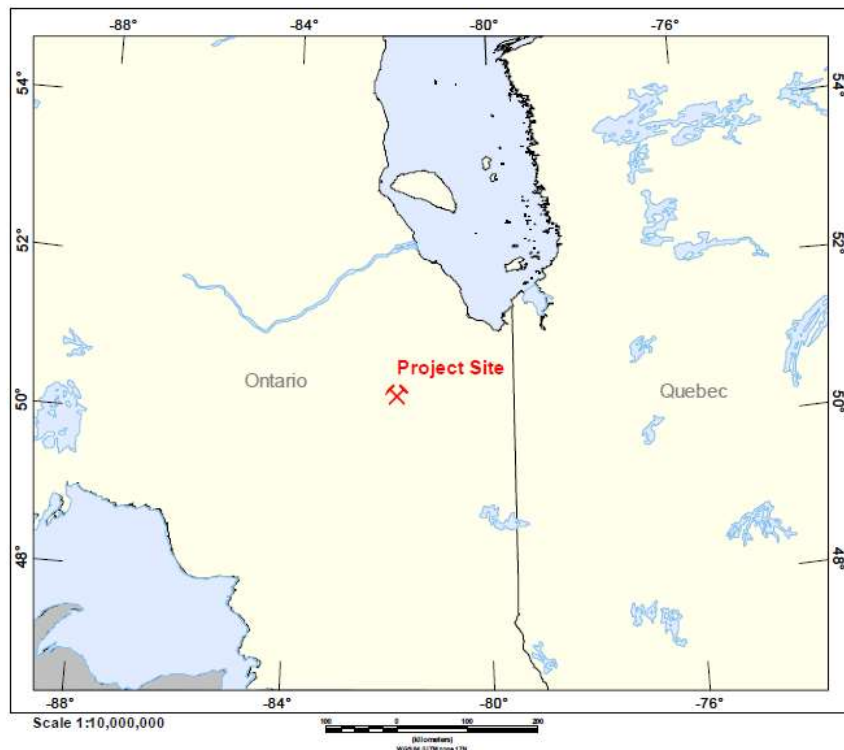


Figure 1: Survey location

1.2 SURVEY AND SYSTEM SPECIFICATIONS

The survey area is located approximately 20 km northwest of Otter Rapids, Ontario (Figure 2).

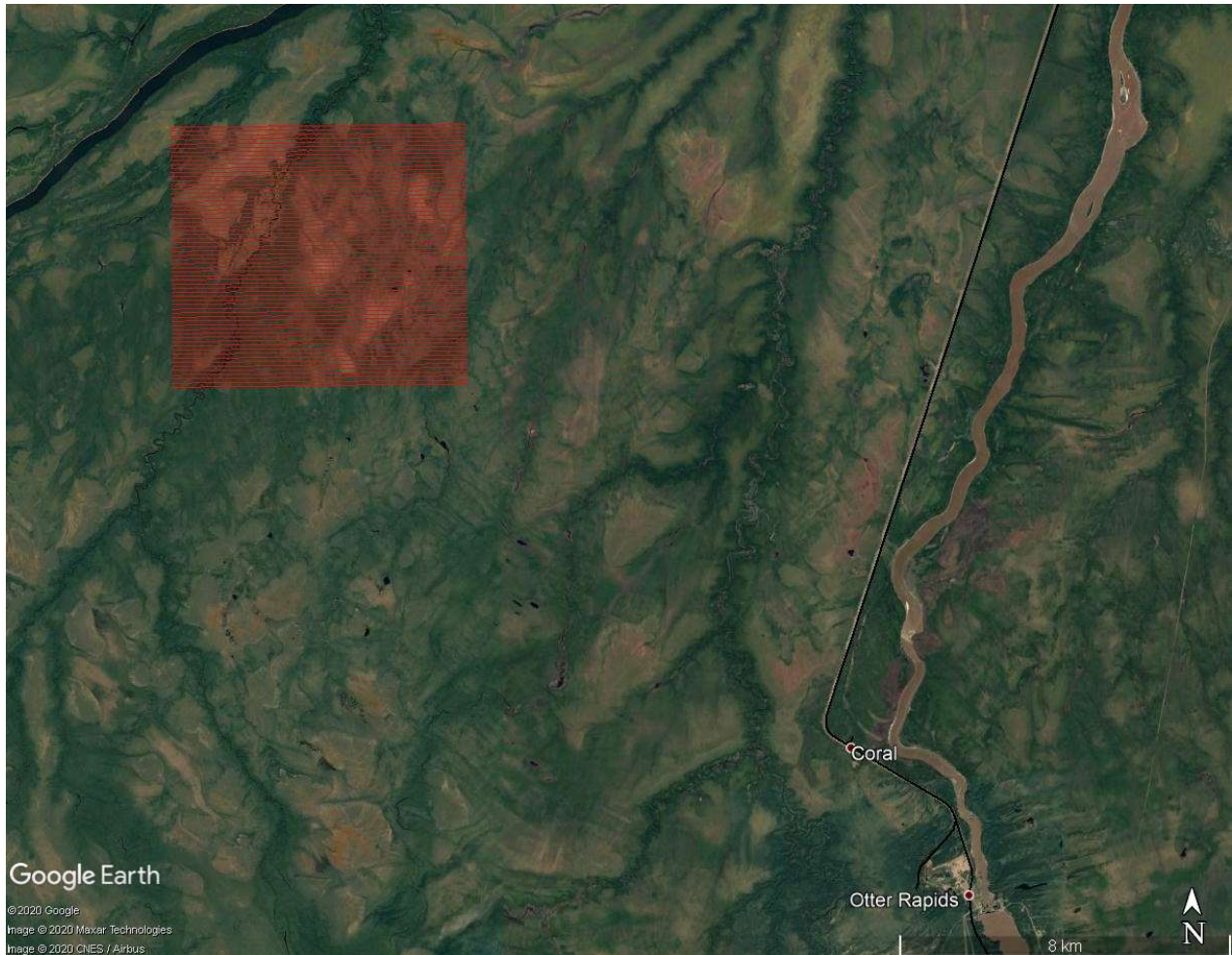


Figure 2: Survey area location on Google Earth.

The survey area consisted of one block flown in west to east ($N 90^{\circ} E$ azimuth) direction, with traverse line spacing of 100 metres, as depicted in **Error! Reference source not found.** Tie lines were neither planned nor flown. For more detailed information on the flight spacing and direction, see Table 1.

1.3 TOPOGRAPHIC RELIEF AND CULTURAL FEATURES

Topographically, the survey area exhibit elevations ranging from 80 to 106 metres and cover an area of 45 square kilometres (**Error! Reference source not found.**).

There are some lakes, rivers, and streams in the survey area. There are no visible signs of culture such as roads, trails or power lines that run through or near the survey area.



Figure 3: Flight path over a Google Earth Image.

2. DATA ACQUISITION

2.1 SURVEY AREA

The survey areas (see **Error! Reference source not found.** and Appendix A) and general flight specifications are as follows:

Table 1: Survey Specifications

Survey block	Line spacing (m)	Area (Km ²)	Planned ¹ Line-km	Actual Line-km	Flight direction	Line numbers
Hecla-Kilmer	Traverse: 100	45	448	459	N 90° E / N 270° E	L1000 – L1630
	Tie: N/A				N/A	N/A
		45	448	459		

Survey area boundaries co-ordinates are provided in Appendix B.

2.2 SURVEY OPERATIONS

Survey operations were based out of Kapuskasing, Ontario. The following table shows the timing of the flying.

Table 2: Survey schedule

Date	Comments
6/30/2020	Mobilization to site
7/1/2020	Reconnaissance flight, set up fuel cache and base station
7/2/2020	Standby due to weather
7/3/2020	Production flights - 329 km flown
7/4/2020	Production flight - 119 km flown
7/5/2020	Flight Path complete, start demobilization
7/6/2020	Demobilization

2.3 FLIGHT SPECIFICATIONS

During the survey, the helicopter was maintained at a mean altitude of 77 metres above the ground with an average survey speed of 101 km/hour. This allowed for an actual average transmitter-receiver loop terrain clearance of 43 metres.

The on-board operator was responsible for monitoring the system integrity. He also maintained a detailed flight log during the survey, tracking the times of the flight as well as any unusual geophysical or topographic features.

On return of the aircrew to the base camp the survey data were transferred from a compact flash card (PCMCIA) to the data processing computer. The data were then uploaded via ftp to the Geotech office in Aurora for daily quality assurance and quality control by qualified personnel.

¹ Note: Actual Line kilometres represent the total line kilometres in the final database. These line-km normally exceed the Planned Line-km, as indicated in the survey NAV files.

2.4 AIRCRAFT AND EQUIPMENT

2.4.1 SURVEY AIRCRAFT

The survey was flown using a Eurocopter Aerospatiale (A-star) 350 B3 helicopter, registration C-FVTM. The helicopter is owned and operated by Geotech Aviation Ltd. Installation of the geophysical and ancillary equipment was carried out by a Geotech Ltd crew.

2.4.2 ELECTROMAGNETIC SYSTEM

The electromagnetic system was a Geotech Time Domain EM (VTEM™ Plus) full receiver-waveform streamed data recorded system. The “full waveform VTEM system” uses the streamed half-cycle recording of transmitter and receiver waveforms to obtain a complete system response calibration throughout the entire survey flight. The VTEM™ system with the Serial number 10 had been used for the survey. The VTEM™ transmitter current waveform is shown diagrammatically in Figure 4.

The VTEM™ Receiver and transmitter coils were in concentric-coplanar and Z-direction oriented configuration. The receiver system for the project also included coincident-coaxial X-direction and Y-direction coils to measure the in-line and cross-line dB/dt and calculate B-Field responses, respectively. The transmitter-receiver loop was towed at a mean distance of 34 metres below the aircraft as shown in Figure 5.

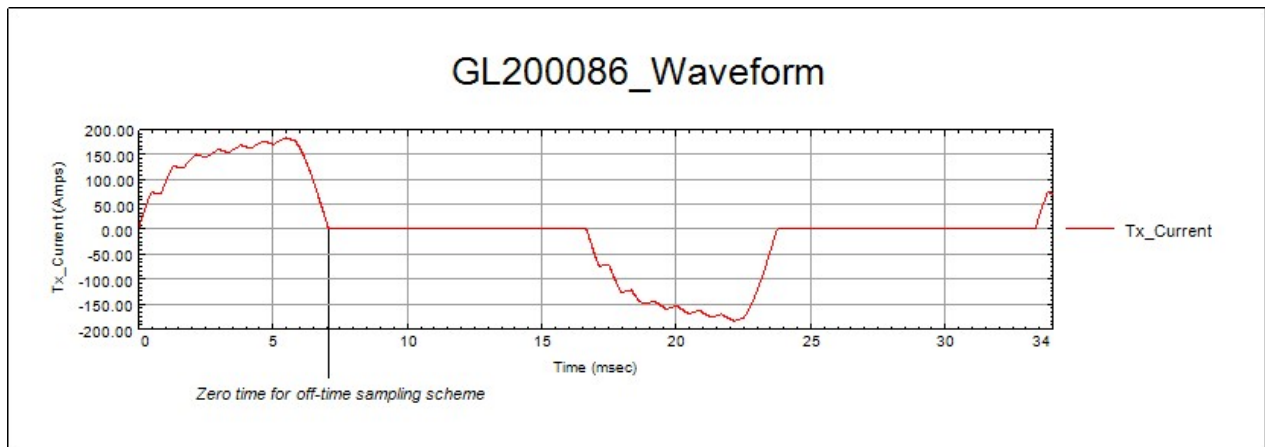


Figure 4: VTEM™plus Transmitter Current Waveform

The VTEM™ decay sampling scheme is shown in Table 3 below. Forty-three time measurement gates were used for the final data processing in the range from 0.021 to 8.083 msec. Zero time for the off-time sampling scheme is equal to the current pulse width and is defined as the time near the end of the turn-off ramp where the dI/dt waveform falls to 1/2 of its peak value.

Table 3: Off-Time Decay Sampling Scheme

VTEM™ Decay Sampling Scheme				
Index	Start	End	Middle	Width
Milliseconds				
4	0.018	0.023	0.021	0.005
5	0.023	0.029	0.026	0.005
6	0.029	0.034	0.031	0.005
7	0.034	0.039	0.036	0.005
8	0.039	0.045	0.042	0.006
9	0.045	0.051	0.048	0.007
10	0.051	0.059	0.055	0.008
11	0.059	0.068	0.063	0.009
12	0.068	0.078	0.073	0.010
13	0.078	0.090	0.083	0.012
14	0.090	0.103	0.096	0.013
15	0.103	0.118	0.110	0.015
16	0.118	0.136	0.126	0.018
17	0.136	0.156	0.145	0.020
18	0.156	0.179	0.167	0.023
19	0.179	0.206	0.192	0.027
20	0.206	0.236	0.220	0.030
21	0.236	0.271	0.253	0.035
22	0.271	0.312	0.290	0.040
23	0.312	0.358	0.333	0.046
24	0.358	0.411	0.383	0.053
25	0.411	0.472	0.440	0.061
26	0.472	0.543	0.505	0.070
27	0.543	0.623	0.580	0.081
28	0.623	0.716	0.667	0.093
29	0.716	0.823	0.766	0.107
30	0.823	0.945	0.880	0.122
31	0.945	1.086	1.010	0.141
32	1.086	1.247	1.161	0.161
33	1.247	1.432	1.333	0.185
34	1.432	1.646	1.531	0.214
35	1.646	1.891	1.760	0.245
36	1.891	2.172	2.021	0.281
37	2.172	2.495	2.323	0.323

VTEM™ Decay Sampling Scheme				
Index	Start	End	Middle	Width
Milliseconds				
38	2.495	2.865	2.667	0.370
39	2.865	3.292	3.063	0.427
40	3.292	3.781	3.521	0.490
41	3.781	4.341	4.042	0.560
42	4.341	4.987	4.641	0.646
43	4.987	5.729	5.333	0.742
44	5.729	6.581	6.125	0.852
45	6.581	7.560	7.036	0.979
46	7.560	8.685	8.083	1.125

Z Component: 4 - 46 time gates
X Component: 20 - 46 time gates
Y Component: 20 - 46 time gates

VTEM™ system specifications:

Transmitter	Receiver
<ul style="list-style-type: none"> • Transmitter loop diameter: 26 m • Number of turns: 4 • Effective Transmitter loop area: 2124 m² • Transmitter base frequency: 30 Hz • Peak current: 184 A • Pulse width: 7.07 ms • Waveform shape: Bi-polar trapezoid • Peak dipole moment: 390,551 nIA • Average transmitter-receiver loop terrain clearance: 44 metres 	<ul style="list-style-type: none"> • X Coil diameter: 0.32 m • Number of turns: 245 • Effective coil area: 19.69 m² • Y Coil diameter: 0.32 m • Number of turns: 245 • Effective coil area: 19.69 m² • Z-Coil diameter: 1.2 m • Number of turns: 100 • Effective coil area: 113.04 m²

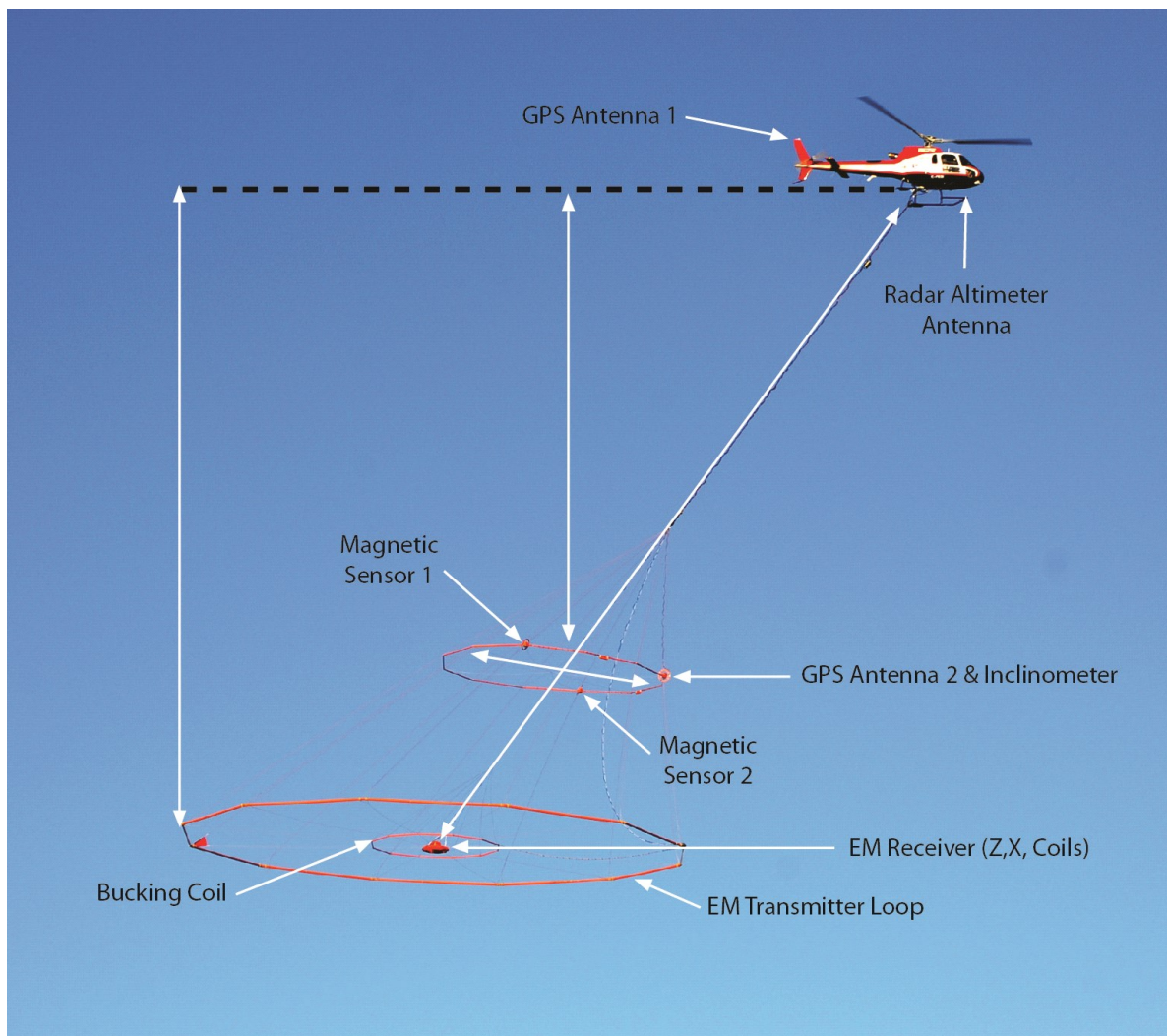


Figure 5: VTEM™plus System Configuration.

2.4.3 FULL WAVEFORM VTEM™ SENSOR CALIBRATION

The calibration is performed on the complete VTEM™ system installed in and connected to the helicopter, using special calibration equipment. This calibration takes place on the ground at the start of the project prior to surveying.

The procedure takes half-cycle files acquired and calculates a calibration file consisting of a single stacked half-cycle waveform. The purpose of the stacking is to attenuate natural and man-made magnetic signals, leaving only the response to the calibration signal.

This calibration allows the transfer function between the EM receiver and data acquisition system and also the transfer function of the current monitor and data acquisition system to be determined. These calibration results are then used in VTEM full waveform processing.

2.4.4 RADAR ALTIMETER

A Terra TRA 3000/TRI 40 radar altimeter was used to record terrain clearance. The antenna was mounted beneath the bubble of the helicopter cockpit (Figure 5).

2.4.5 GPS NAVIGATION SYSTEM

The navigation system used was a Geotech PC104 based navigation system utilizing a NovAtel's WAAS (Wide Area Augmentation System) enabled GPS receiver, Geotech navigate software, a full screen display with controls in front of the pilot to direct the flight and a NovAtel GPS antenna mounted on the helicopter tail (Figure 5). As many as 11 GPS and two WAAS satellites may be monitored at any time. The positional accuracy or circular error probability (CEP) is 1.8 m, with WAAS active, it is 1.0 m. The co-ordinates of the survey area were set-up prior to the survey and the information was fed into the airborne navigation system. The second GPS antenna is installed on the additional magnetic loop together with Gyro Inclinometer.

2.4.6 DIGITAL ACQUISITION SYSTEM

A Geotech data acquisition system recorded the digital survey data on an internal compact flash card. Data are displayed on an LCD screen as traces to allow the operator to monitor the integrity of the system. The data type and sampling interval as provided in Table 4

Table 4: Acquisition Sampling Rates

Data Type	Sampling
TDEM	0.1 sec
GPS Position	0.2 sec
Radar Altimeter	0.2 sec

3. PERSONNEL

The following Geotech Ltd. personnel were involved in the project.

FIELD:

Project Manager:	TaiChyi Shei (Office)
Data QC:	Nick Venter
Crew chief:	Gary Bissonnette
Operator:	Roberto DiBari

The survey pilot and the mechanical engineer were employed directly by the helicopter operator – Geotech Aviation.

Pilot:	Robert Fauteux
Mechanical Engineer:	Ian Boychuck

OFFICE:

Preliminary Data Processing:	Nick Venter
Final Data Processing:	Emily Data
Data QA/QC:	Keeme Mokubung Jean M. Legault
Reporting/Mapping:	Joseli Soares

Processing and Interpretation phases were carried out under the supervision of Keeme Mokubung & Jean M. Legault, M.Sc.A, P.Eng, and P.Geo - Chief Geophysicist. The customer relations were looked after by David Hitz, Client Relationship Manager.

4. DATA PROCESSING AND PRESENTATION

Data compilation and processing were carried out by the application of Geosoft OASIS Montaj and programs proprietary to Geotech Ltd.

4.1 FLIGHT PATH

The flight path, recorded by the acquisition program as WGS84 latitude/longitude, was converted into the WGS84 Datum, UTM Zone 17N coordinate system in Oasis Montaj.

The flight path was drawn using linear interpolation between x and y positions from the navigation system. Positions are updated every second and expressed as UTM easting's (x) and UTM northing's (y).

4.2 ELECTROMAGNETIC DATA

The Full Waveform EM specific data processing operations included:

- Half cycle stacking (performed at time of acquisition);
- System response correction;
- Parasitic and drift removal.

A three-stage digital filtering process was used to reject major sferic events and to reduce noise levels. Local sferic activity can produce sharp, large amplitude events that cannot be removed by conventional filtering procedures. Smoothing or stacking will reduce their amplitude but leave a broader residual response that can be confused with geological phenomena. To avoid this possibility, a computer algorithm searches out and rejects the major sferic events.

The signal to noise ratio was further improved by the application of a low pass linear digital filter. This filter has zero phase shift, which prevents any lag or peak displacement from occurring, and it suppresses only variations with a wavelength less than about 1 second or 15 metres. This filter is a symmetrical 1 sec linear filter.

The results are presented as stacked profiles of EM decays for the time gates, in linear - logarithmic scale for the B-field Z component and dB/dt responses for the Z and X components. B-field Z component time channels recorded at 0.880 milliseconds after the termination of the impulse is also presented as a colour image. Calculated Time Constant (TAU) is presented in Appendix C. Resistivity Depth Image (RDI) is also presented in Appendix F and G.

VTEM™ has up to three receiver coil orientations. The Z-axis coil is oriented parallel to the transmitter coil axis and both are horizontal to the ground. The X-axis coil is oriented parallel to the ground and along the flight-line direction. The Y-axis coil is oriented parallel to the ground and perpendicular to the flight-line direction. The combination of the X, Y and Z coils configuration provides information on the position, depth, dip and thickness of a conductor. Generalized modeling results of VTEM data, are shown in Appendix D.

In general, X-component data produce cross-over type anomalies: from “+ to -” in flight direction of flight for “thin” sub vertical targets and from “- to +” in direction of flight for “thick” targets. Z component data produce double peak type anomalies for “thin” sub vertical targets and single peak for “thick” targets.

The limits and change-over of “thin-thick” depends on the dimensions of the TEM system (Appendix D, Figure D-16).

Due to the fact that the X component polarity is depends on the flight line direction, a convolution Fraser Filter (Figure 6) is applied to X component data to assist in defining the axes of conductors on a gridded contour map form. In this case positive FF anomalies always correspond to “plus-to-minus” X data crossovers, for thin-type conductors, which are independent of the flight line direction. Conversely, thick-type conductors that correspond to “minus-to-plus” X data crossovers are identified with negative FF anomalies.

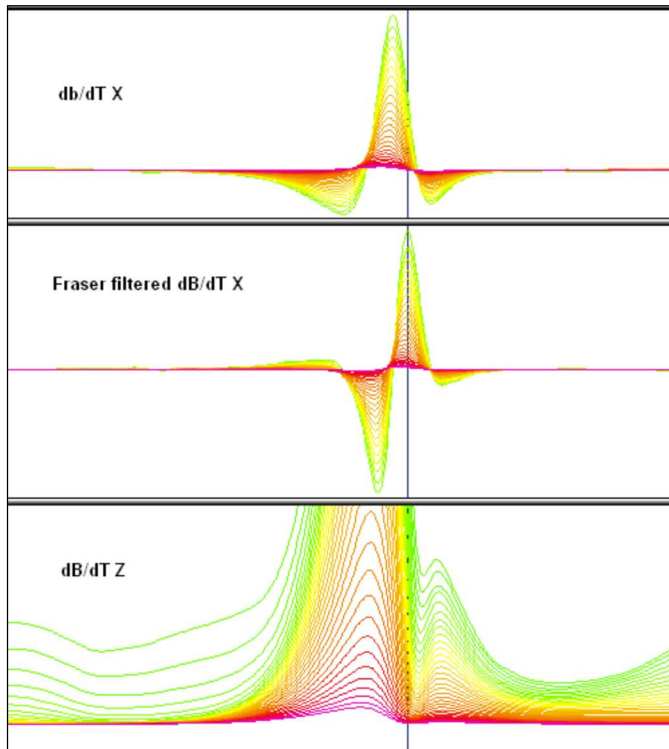


Figure 6: Z, X and Fraser filtered X (FFx) components for “thin” target.

5. DELIVERABLES

5.1 SURVEY REPORT

The survey report describes the data acquisition, processing, and final presentation of the survey results. The survey report is provided in two paper copies and digitally in PDF format.

5.2 MAPS

Final maps were produced at scale of 1:10,000 for best representation of the survey size and line spacing. The coordinate/projection system used was WGS84 Datum, UTM Zone 17N. All maps show the flight path trace and topographic data; latitude and longitude are also noted on maps.

The preliminary and final results of the survey are presented as EM profiles, an early, middle, and late-time gate gridded EM channel.

- Maps at 1:10,000 in Geosoft MAP format, as follows:

GL200086_10k_dBdt:	dB/dt profiles Z Component, Time Gates 0.220 – 7.036 ms in linear – logarithmic scale.
GL200086_10k_BField:	B-field profiles Z Component, Time Gates 0.220 – 7.036 ms in linear – logarithmic scale.
GL200086_10k_BFz30:	B-field Z Component Channel 30, Time Gate 0.880 ms colour image.
GL200086_10k_SFz15:	VTEM dB/dt Z Component Channel 15, Time Gate 0.110 ms.
GL200086_10k_SFz25:	VTEM dB/dt Z Component Channel 25, Time Gate 0.440 ms.
GL200086_10k_SFz35:	VTEM dB/dt Z Component Channel 35, Time Gate 1.760 ms.
GL200086_10k_SFxFF25:	Fraser Filtered dB/dt X Component Channel 25, Time Gate 0.440 ms colour image.
GL200086_10k_TauSF:	dB/dt Calculated Time Constant (Tau)

- Maps are also presented in PDF format.
- The topographic data base was derived from 1:50,000 CANVEC data and Geocommunities: www.geocomm.com
- A Google Earth file *GL200086_VR.kmz* showing the flight path of the block is included. Free versions of Google Earth software from: <http://earth.google.com/download-earth.html>

5.3 DIGITAL DATA

Two copies of the data and maps on DVD were prepared to accompany the report. Each DVD contains a digital file of the line data in GDB Geosoft Montaj format as well as the maps in Geosoft Montaj Map and PDF format.

5.3.1 DVD STRUCTURE

Data contains databases, grids and maps, as described below.
 Report contains a copy of the report and appendices in PDF format.

Databases in Geosoft GDB format, containing the channels listed in Table 5.

Table 5: Geosoft GDB Data Format

Channel name	Units	Description
X:	metres	Easting WGS84 Zone 17N
Y:	metres	Northing WGS84 Zone 17N
Longitude:	Decimal Degrees	WGS84 Longitude data
Latitude:	Decimal Degrees	WGS84 Latitude data
Z:	metres	GPS antenna elevation (above Geoid)
Zb:	metres	EM bird elevation (above Geoid)
Radar:	metres	Helicopter terrain clearance from radar altimeter
Radarb:	metres	Calculated EM transmitter-receiver loop terrain clearance from radar altimeter
DEM:	metres	Digital Elevation Model
Gtime:	Seconds of the day	GPS time
SFz[4]:	pV/(A*m ⁴)	Z dB/dt 0.021 millisecond time channel
SFz[5]:	pV/(A*m ⁴)	Z dB/dt 0.026 millisecond time channel
SFz[6]:	pV/(A*m ⁴)	Z dB/dt 0.031 millisecond time channel
SFz[7]:	pV/(A*m ⁴)	Z dB/dt 0.036 millisecond time channel
SFz[8]:	pV/(A*m ⁴)	Z dB/dt 0.042 millisecond time channel
SFz[9]:	pV/(A*m ⁴)	Z dB/dt 0.048 millisecond time channel
SFz[10]:	pV/(A*m ⁴)	Z dB/dt 0.055 millisecond time channel
SFz[11]:	pV/(A*m ⁴)	Z dB/dt 0.063 millisecond time channel
SFz[12]:	pV/(A*m ⁴)	Z dB/dt 0.073 millisecond time channel
SFz[13]:	pV/(A*m ⁴)	Z dB/dt 0.083 millisecond time channel
SFz[14]:	pV/(A*m ⁴)	Z dB/dt 0.096 millisecond time channel
SFz[15]:	pV/(A*m ⁴)	Z dB/dt 0.110 millisecond time channel
SFz[16]:	pV/(A*m ⁴)	Z dB/dt 0.126 millisecond time channel
SFz[17]:	pV/(A*m ⁴)	Z dB/dt 0.145 millisecond time channel
SFz[18]:	pV/(A*m ⁴)	Z dB/dt 0.167 millisecond time channel
SFz[19]:	pV/(A*m ⁴)	Z dB/dt 0.192 millisecond time channel
SFz[20]:	pV/(A*m ⁴)	Z dB/dt 0.220 millisecond time channel
SFz[21]:	pV/(A*m ⁴)	Z dB/dt 0.253 millisecond time channel
SFz[22]:	pV/(A*m ⁴)	Z dB/dt 0.290 millisecond time channel
SFz[23]:	pV/(A*m ⁴)	Z dB/dt 0.333 millisecond time channel
SFz[24]:	pV/(A*m ⁴)	Z dB/dt 0.383 millisecond time channel
SFz[25]:	pV/(A*m ⁴)	Z dB/dt 0.440 millisecond time channel
SFz[26]:	pV/(A*m ⁴)	Z dB/dt 0.505 millisecond time channel

Channel name	Units	Description
SFz[27]:	pV/(A*m ⁴)	Z dB/dt 0.580 millisecond time channel
SFz[28]:	pV/(A*m ⁴)	Z dB/dt 0.667 millisecond time channel
SFz[29]:	pV/(A*m ⁴)	Z dB/dt 0.766 millisecond time channel
SFz[30]:	pV/(A*m ⁴)	Z dB/dt 0.880 millisecond time channel
SFz[31]:	pV/(A*m ⁴)	Z dB/dt 1.010 millisecond time channel
SFz[32]:	pV/(A*m ⁴)	Z dB/dt 1.161 millisecond time channel
SFz[33]:	pV/(A*m ⁴)	Z dB/dt 1.333 millisecond time channel
SFz[34]:	pV/(A*m ⁴)	Z dB/dt 1.531 millisecond time channel
SFz[35]:	pV/(A*m ⁴)	Z dB/dt 1.760 millisecond time channel
SFz[36]:	pV/(A*m ⁴)	Z dB/dt 2.021 millisecond time channel
SFz[37]:	pV/(A*m ⁴)	Z dB/dt 2.323 millisecond time channel
SFz[38]:	pV/(A*m ⁴)	Z dB/dt 2.667 millisecond time channel
SFz[39]:	pV/(A*m ⁴)	Z dB/dt 3.063 millisecond time channel
SFz[40]:	pV/(A*m ⁴)	Z dB/dt 3.521 millisecond time channel
SFz[41]:	pV/(A*m ⁴)	Z dB/dt 4.042 millisecond time channel
SFz[42]:	pV/(A*m ⁴)	Z dB/dt 4.641 millisecond time channel
SFz[43]:	pV/(A*m ⁴)	Z dB/dt 5.333 millisecond time channel
SFz[44]:	pV/(A*m ⁴)	Z dB/dt 6.125 millisecond time channel
SFz[45]:	pV/(A*m ⁴)	Z dB/dt 7.036 millisecond time channel
SFz[46]:	pV/(A*m ⁴)	Z dB/dt 8.083 millisecond time channel
SFx[20]:	pV/(A*m ⁴)	X dB/dt 0.220 millisecond time channel
SFx[21]:	pV/(A*m ⁴)	X dB/dt 0.253 millisecond time channel
SFx[22]:	pV/(A*m ⁴)	X dB/dt 0.290 millisecond time channel
SFx[23]:	pV/(A*m ⁴)	X dB/dt 0.333 millisecond time channel
SFx[24]:	pV/(A*m ⁴)	X dB/dt 0.383 millisecond time channel
SFx[25]:	pV/(A*m ⁴)	X dB/dt 0.440 millisecond time channel
SFx[26]:	pV/(A*m ⁴)	X dB/dt 0.505 millisecond time channel
SFx[27]:	pV/(A*m ⁴)	X dB/dt 0.580 millisecond time channel
SFx[28]:	pV/(A*m ⁴)	X dB/dt 0.667 millisecond time channel
SFx[29]:	pV/(A*m ⁴)	X dB/dt 0.766 millisecond time channel
SFx[30]:	pV/(A*m ⁴)	X dB/dt 0.880 millisecond time channel
SFx[31]:	pV/(A*m ⁴)	X dB/dt 1.010 millisecond time channel
SFx[32]:	pV/(A*m ⁴)	X dB/dt 1.161 millisecond time channel
SFx[33]:	pV/(A*m ⁴)	X dB/dt 1.333 millisecond time channel
SFx[34]:	pV/(A*m ⁴)	X dB/dt 1.531 millisecond time channel
SFx[35]:	pV/(A*m ⁴)	X dB/dt 1.760 millisecond time channel
SFx[36]:	pV/(A*m ⁴)	X dB/dt 2.021 millisecond time channel
SFx[37]:	pV/(A*m ⁴)	X dB/dt 2.323 millisecond time channel
SFx[38]:	pV/(A*m ⁴)	X dB/dt 2.667 millisecond time channel
SFx[39]:	pV/(A*m ⁴)	X dB/dt 3.063 millisecond time channel
SFx[40]:	pV/(A*m ⁴)	X dB/dt 3.521 millisecond time channel
SFx[41]:	pV/(A*m ⁴)	X dB/dt 4.042 millisecond time channel
SFx[42]:	pV/(A*m ⁴)	X dB/dt 4.641 millisecond time channel
SFx[43]:	pV/(A*m ⁴)	X dB/dt 5.333 millisecond time channel
SFx[44]:	pV/(A*m ⁴)	X dB/dt 6.125 millisecond time channel
SFx[45]:	pV/(A*m ⁴)	X dB/dt 7.036 millisecond time channel
SFx[46]:	pV/(A*m ⁴)	X dB/dt 8.083 millisecond time channel
SFy	pV/(A*m ⁴)	Y dB/dt data for time channels 20 to 46
BFz	(pV*ms)/(A*m ⁴)	Z B-Field data for time channels 4 to 46
BFx	(pV*ms)/(A*m ⁴)	X B-Field data for time channels 20 to 46

Channel name	Units	Description
BFy	$(\text{pV}\cdot\text{ms})/(\text{A}\cdot\text{m}^4)$	Y B-Field data for time channels 20 to 46
SFxFF	$\text{pV}/(\text{A}\cdot\text{m}^4)$	Fraser Filtered X dB/dt
NchanBF		Latest time channels of TAU calculation
TauBF	ms	Time constant B-Field
NchanSF		Latest time channels of TAU calculation
TauSF	ms	Time constant dB/dt
PLM:		60 Hz power line monitor

Electromagnetic B-field and dB/dt Z component data are found in array channel format between indexes 4 – 46, with X and Y component data from 20 – 46, as described above.

5.3.2 DATABASE OF THE APPARENT RESISTIVITY DEPTH IMAGING PRODUCTS

- in Geosoft GDB format, containing the following channels:

Table 6: Geosoft Apparent Resistivity Depth Image GDB Data Format

Channel name	Units	Description
Xg	metres	Easting WGS84 Zone 18N
Yg	metres	Northing WGS84 Zone 18N
Dist:	metres	Distance from the beginning of the line
Depth:	metres	Array channel, depth from the surface
Z:	metres	Array channel, depth from sea level
AppRes:	Ohm-m	Array channel, Apparent Resistivity
TR:	metres	EM system height from sea level
Topo:	metres	Digital Elevation Model
Radarb:	metres	Calculated EM transmitter-receiver loop terrain clearance from radar altimeter
SF:	$\text{pV}/(\text{A}\cdot\text{m}^4)$	Array channel, dB/dT
DOI:	metres	Depth of Investigation: a measure of VTEM depth effectiveness
PLM:		60Hz Power Line Monitor

5.3.3 DATABASE OF THE VTEM WAVEFORM

- “GL200086_Waveform.gdb” in Geosoft GDB format, containing the following channels:

Table 7: Geosoft database for the VTEM waveform

Channel name	Units	Description
Time:	milliseconds	Sampling rate interval, 5.2083 microseconds
Tx_Current:	amps	Output current of the transmitter

5.3.4 RESISTIVITY DEPTH IMAGE PRODUCTS

- Sections: Apparent resistivity sections along each line in .GRD and .PDF format
- Slices: Apparent resistivity slices at selected depths from 25m to depth of investigation, at an increment of 25m in .GRD and .PDF format
- Voxel: 3D Voxel imaging of apparent resistivity data clipped by digital elevation and depth of investigation

5.3.5 GRIDS IN GEOSOFT GRD AND GEOTIFF FORMAT

- Listed as follows:

GL200086_BFz30:	B-Field Z Component Channel 30 (Time Gate 0.880ms)
GL200086_DEM:	Digital Elevation Model (m)
GL200086_SFxFF25:	Fraser Filtered dB/dt X, Component Channel 25 (Time Gate 0.440 ms)
GL200086_TauBF:	B-Field Z Component, Calculated Time Constant (ms)
GL200086_TauSF:	dB/dt Z Component, Calculated Time Constant (ms)
GL200086_PLM:	60Hz Power Line Monitor
GL200086_SFz15:	dB/dt Z Component Channel 15 (Time Gate 0.110 ms)
GL200086_SFz25:	dB/dt Z Component Channel 25 (Time Gate 0.440 ms)
GL200086_SFz35:	dB/dt Z Component Channel 35 (Time Gate 1.760 ms)

A Geosoft .GRD file has a .GI metadata file associated with it, containing grid projection information. A grid cell size of 25 metres was used.

6. CONCLUSIONS AND RECOMMENDATIONS

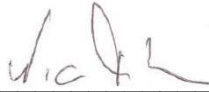
A helicopter-borne versatile time domain electromagnetic (VTEM™ Plus) geophysical survey has been completed over the Hecla-Kilmer property, near Otter Rapids, Ontario.

The total area coverage is 45 km² and the total survey line coverage is 459 line kilometres. The principal sensors included a Time Domain VTEM™ plus system. Results have been presented as stacked profiles and contour colour images at a scale of 1:10,000.

Based on the geophysical results obtained, a number of anomalous zones are identified on the survey block. They indicate the presence of VTEM anomalies that seem to correspond to magnetic lows in the middle of the block, within the Hecla-Kilmer complex. According to the resistivity depth imaging slices, the top of the response sources lies around 50m depth.

The VTEM results may contain worthwhile information in support of exploration for mineral formations. If these conductors correspond to an exploration model, then a detailed interpretation and analysis of the results by performing EM Anomaly Picks, grading and depth estimates, and 1D Inversions are recommended for this project.

Respectfully submitted²,



Nick Venter
Geotech Ltd.



Emily Data
Geotech Ltd.



Jean M. Legault, M.Sc.A, P.Eng, P.Geo.
Geotech Ltd.



Joseli Soares
Geotech Ltd

August 2020.

² Final data processing of the EM data was carried out by Emily Data, from the office of Geotech Ltd. in Aurora, Ontario, under the supervision of Keeme Mokubung and Jean M. Legault, M.Sc.A, P.Eng, and P.Geo - Chief Geophysicist.

APPENDIX A

SURVEY AREA LOCATION MAP



Overview of the Survey Area

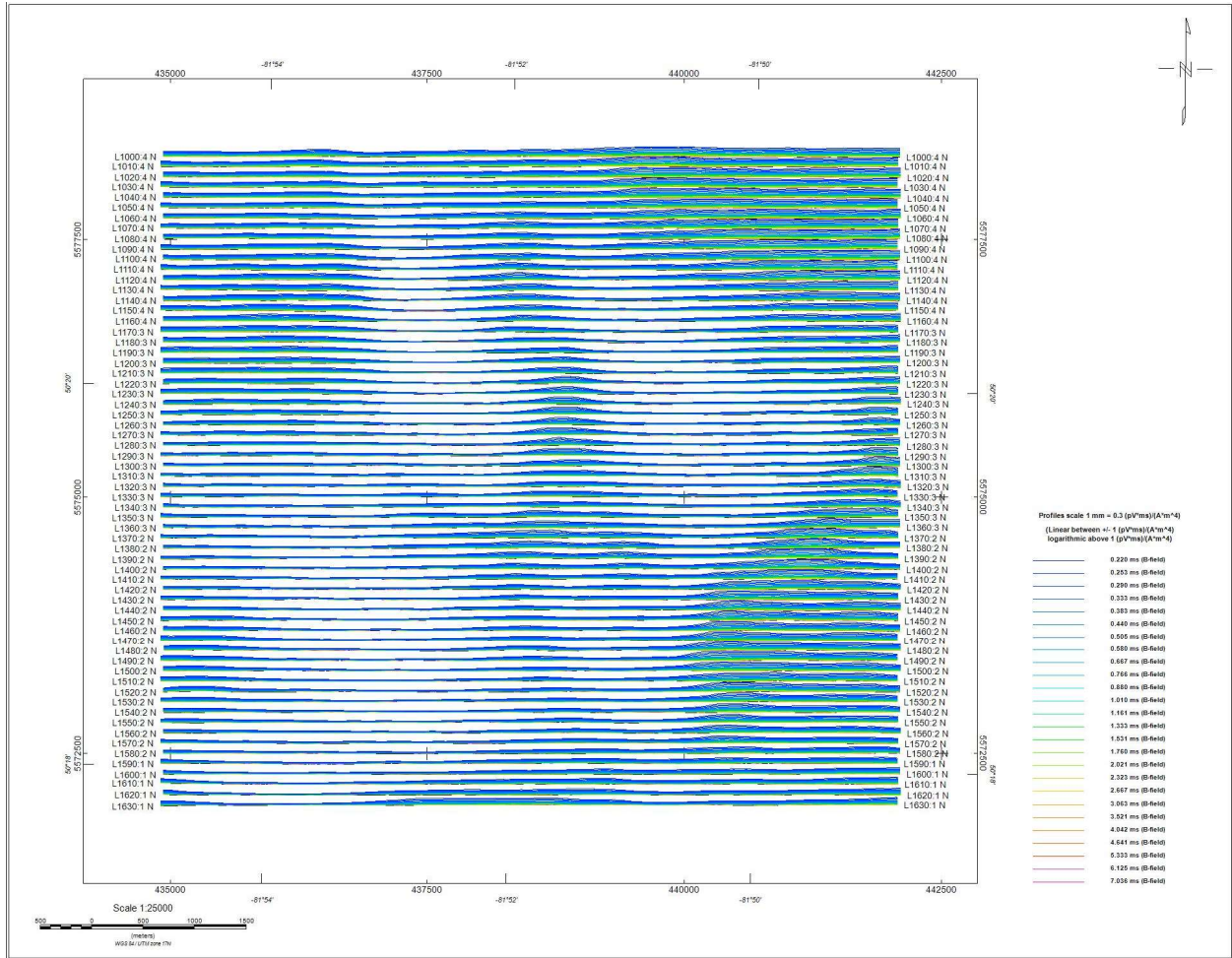
APPENDIX B

SURVEY AREA COORDINATES

(WGS84 UTM Zone 17N)

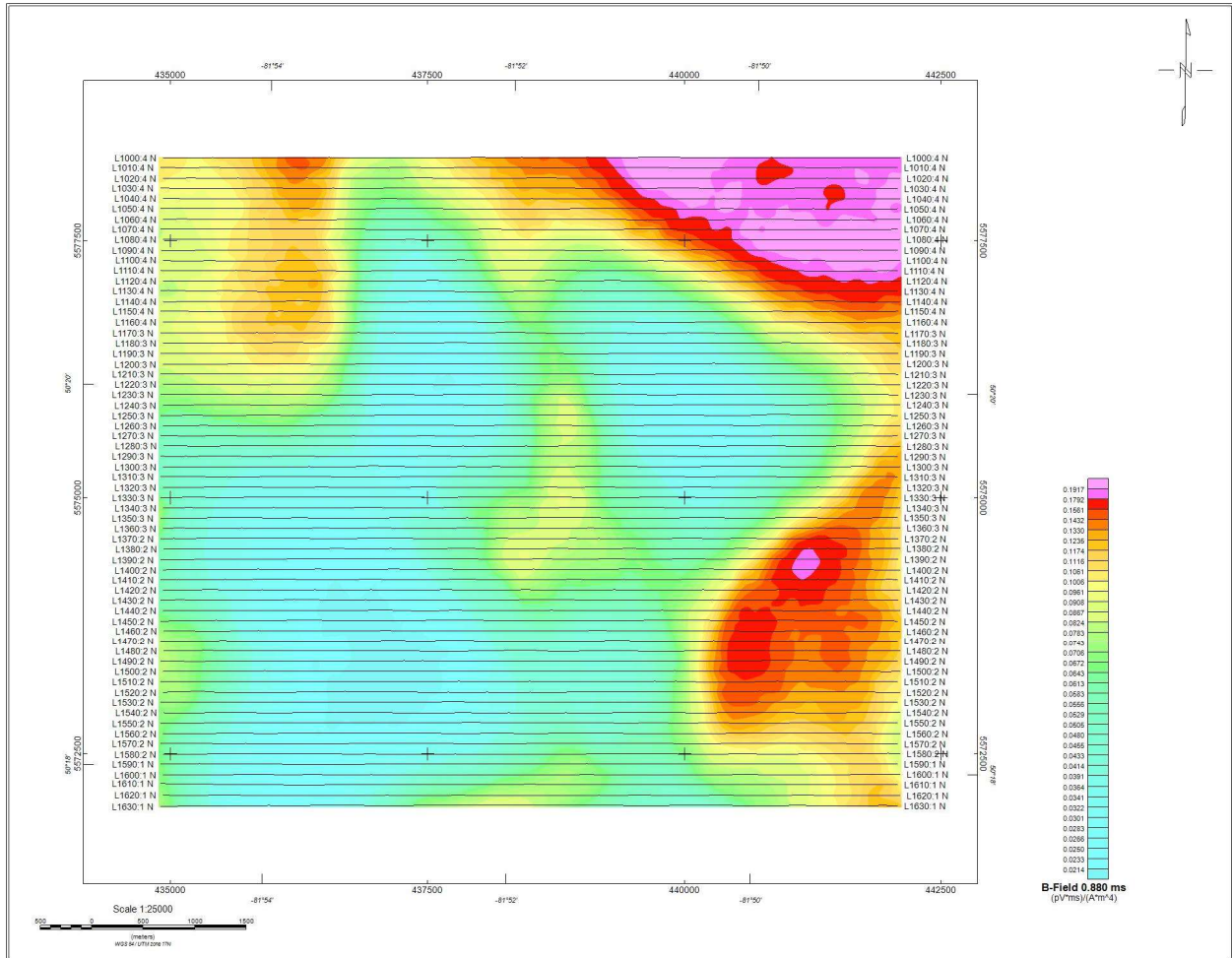
Hecla-Kilmer	
X	Y
434887.5	5571987.5
442112.5	5571987.5
442112.5	5578312.5
434887.5	5578312.5

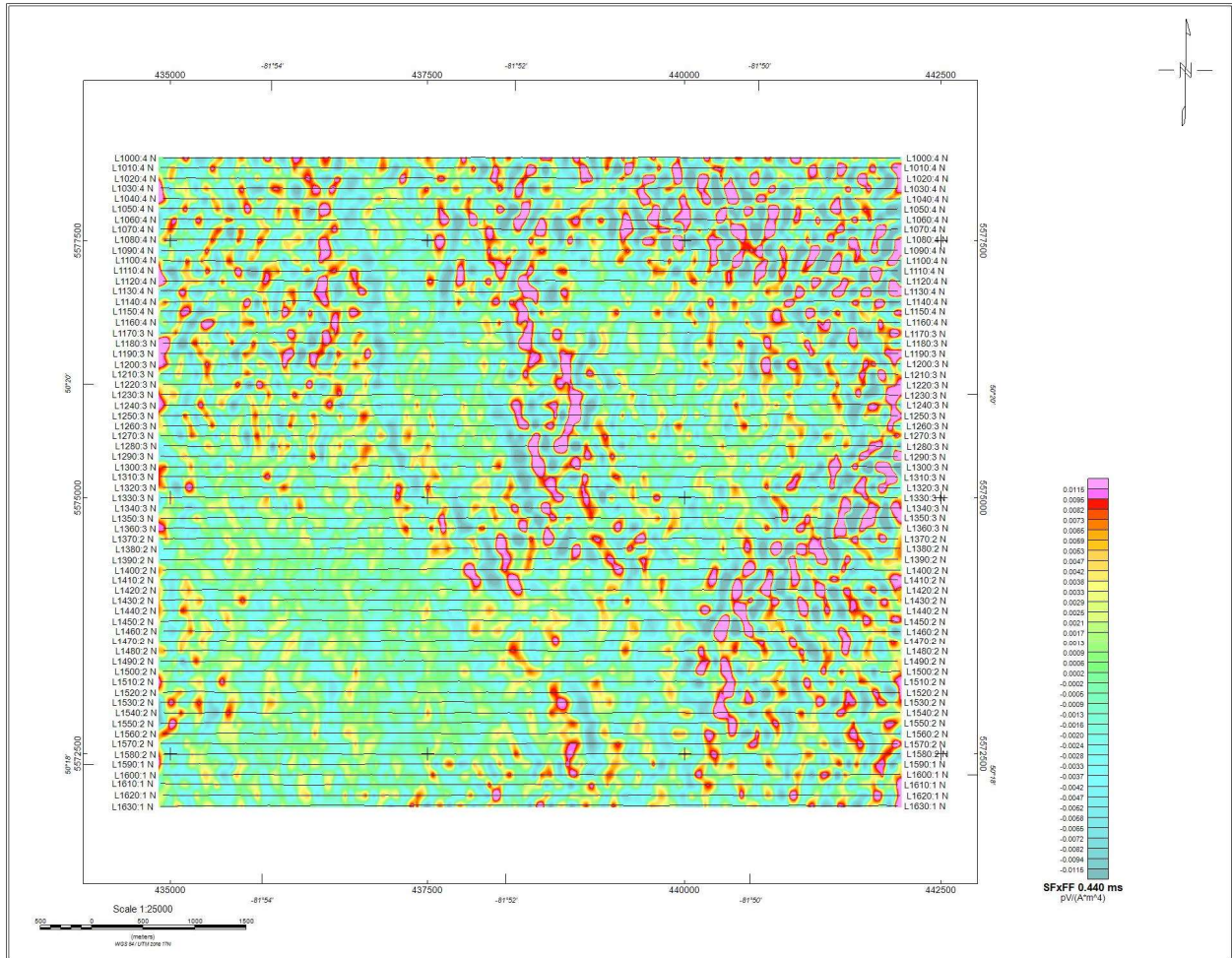
APPENDIX C - GEOPHYSICAL MAPS¹



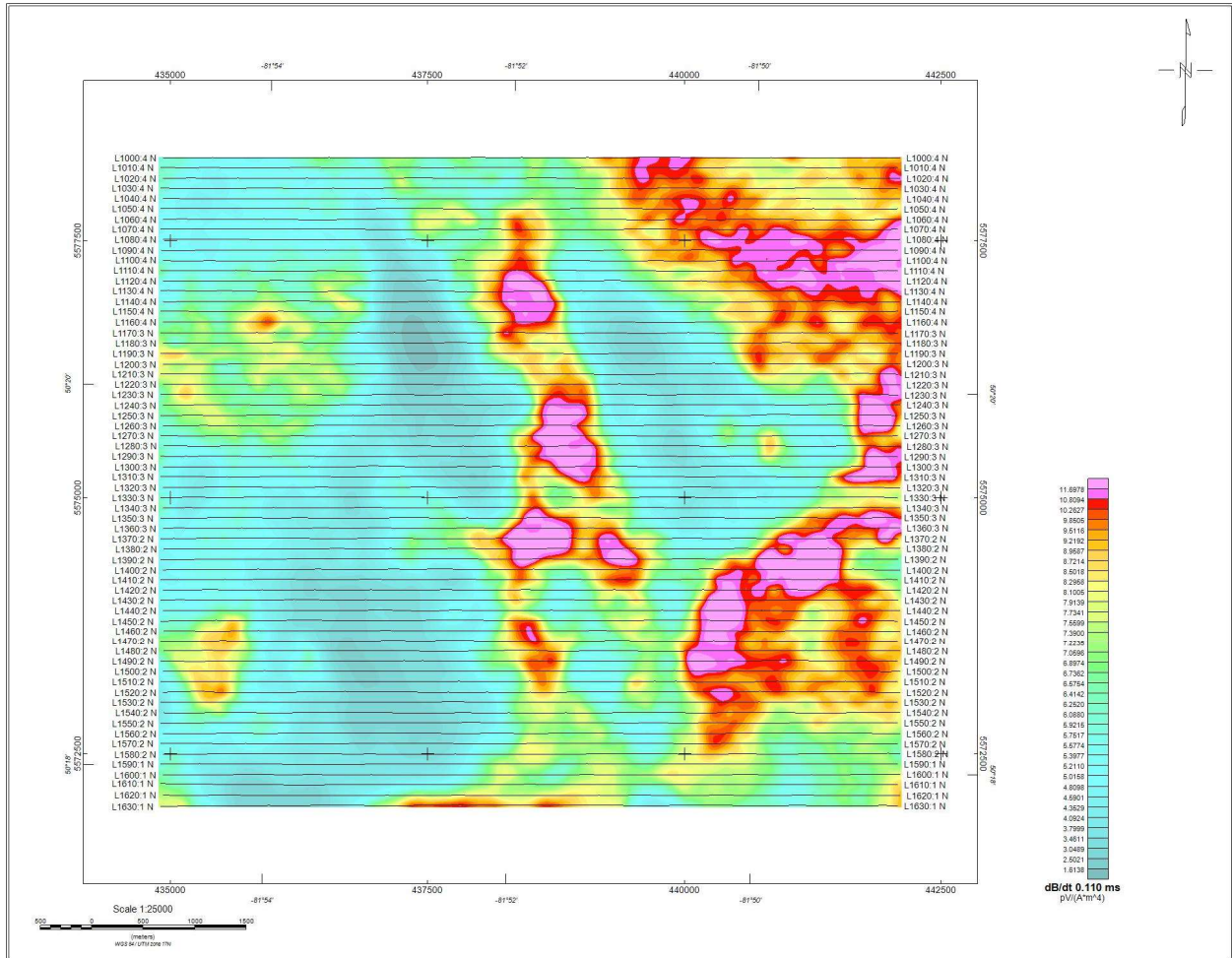
B-field profiles Z Component, Time Gates 0.220 – 7.036 ms

¹ Complete full size geophysical maps are also available in PDF format located in the final data maps folder

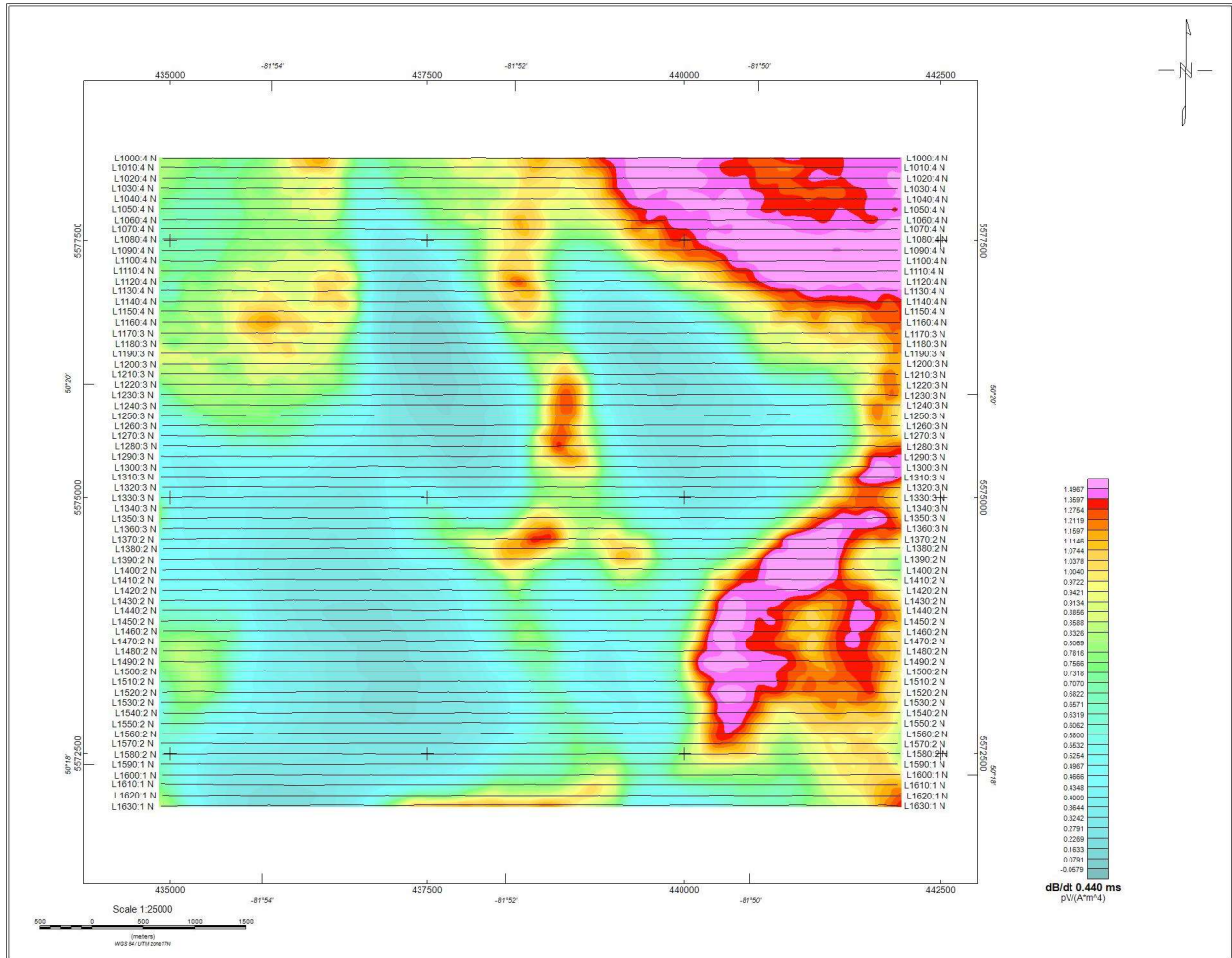




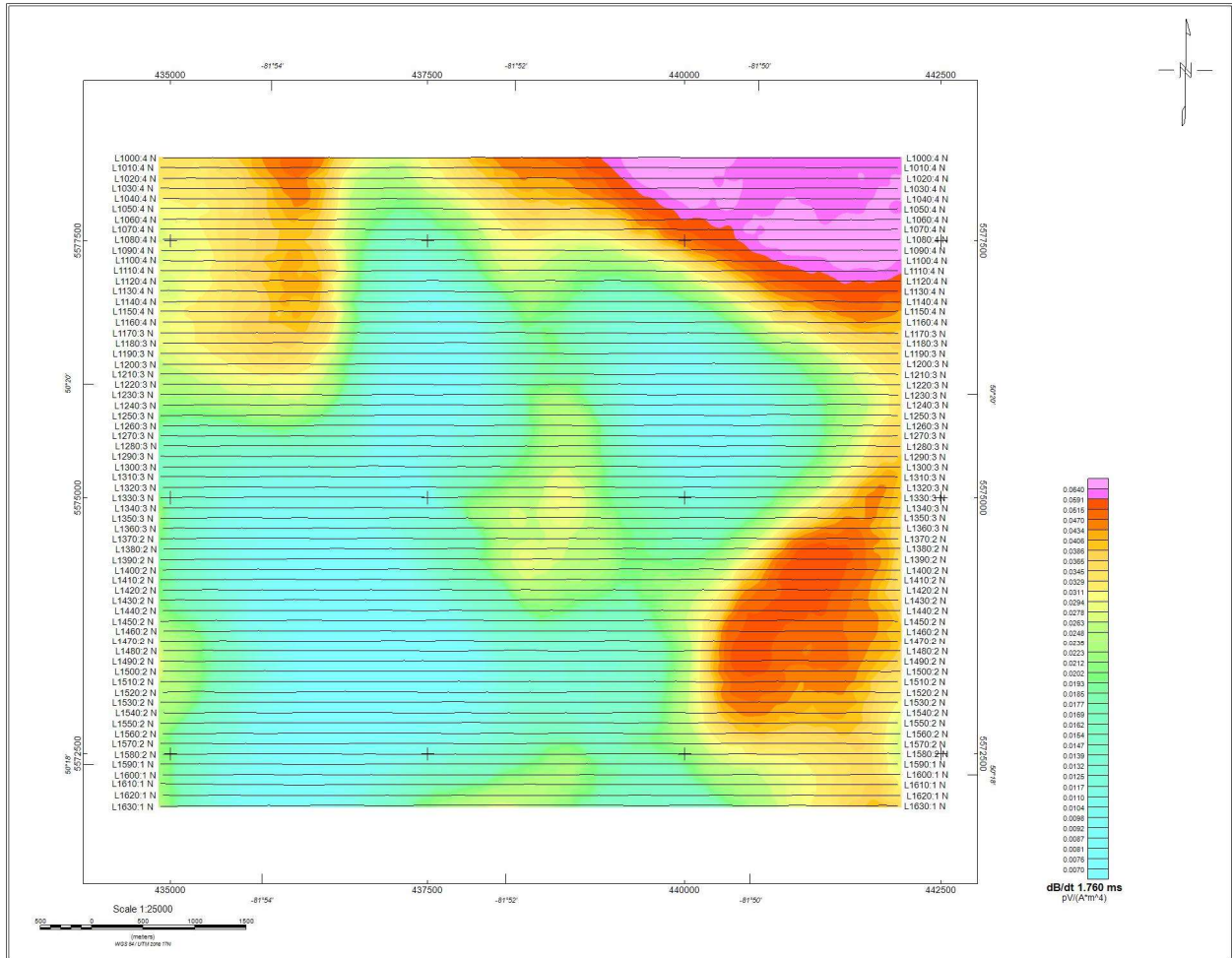
Fraser Filtered dB/dt X Component Channel 25, Time Gate 0.440 ms colour image.



VTEM dB/dt Z Component Channel 15, Time Gate 0.110 ms

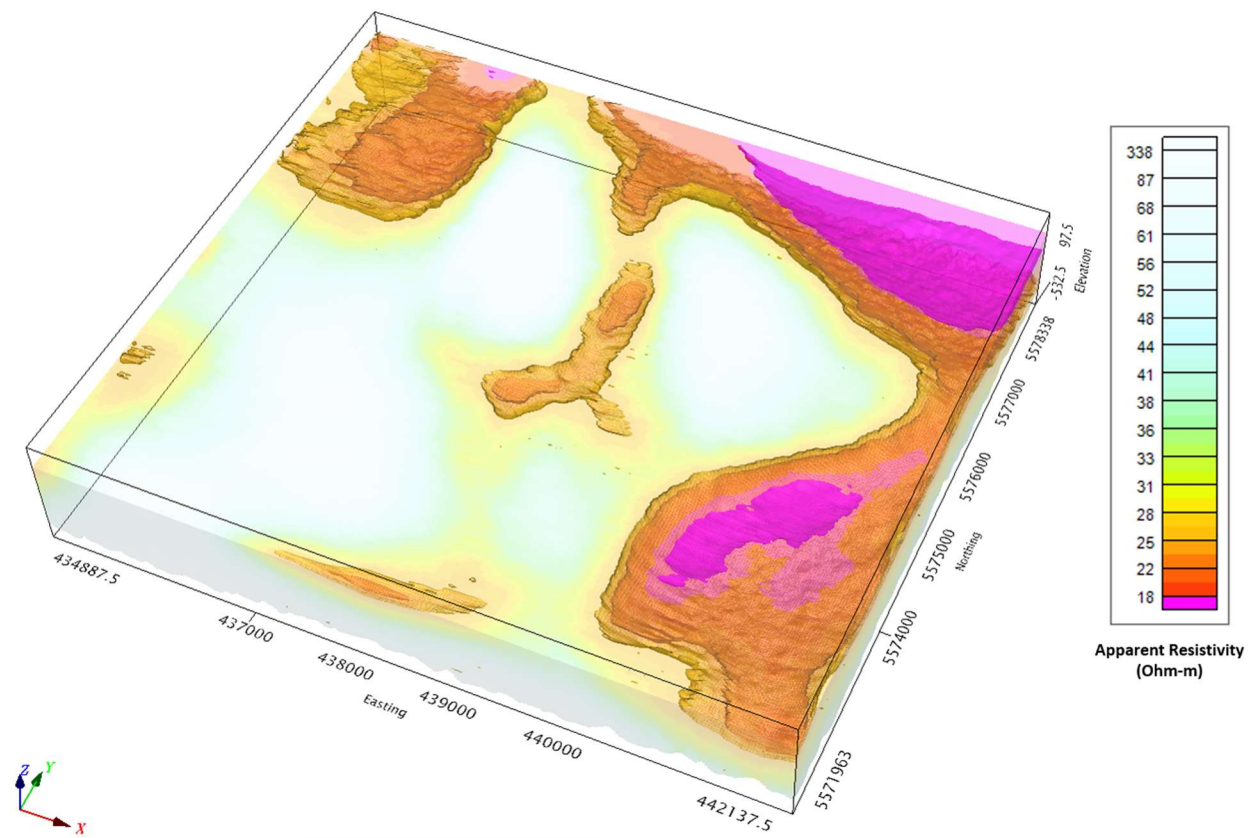


VTEM dB/dt Z Component Channel 25, Time Gate 0.440 ms



VTEM dB/dt Z Component Channel 35, Time Gate 1.760 ms

RESISTIVITY DEPTH IMAGE (RDI) MAP



3D View of RDI Apparent Resistivity Voxel

APPENDIX D

GENERALIZED MODELING RESULTS OF THE VTEM SYSTEM INTRODUCTION

The VTEM system is based on a concentric or central loop design, whereby, the receiver is positioned at the centre of a transmitter loop that produces a primary field. The wave form is a bipolar, modified square wave with a turn-on and turn-off at each end.

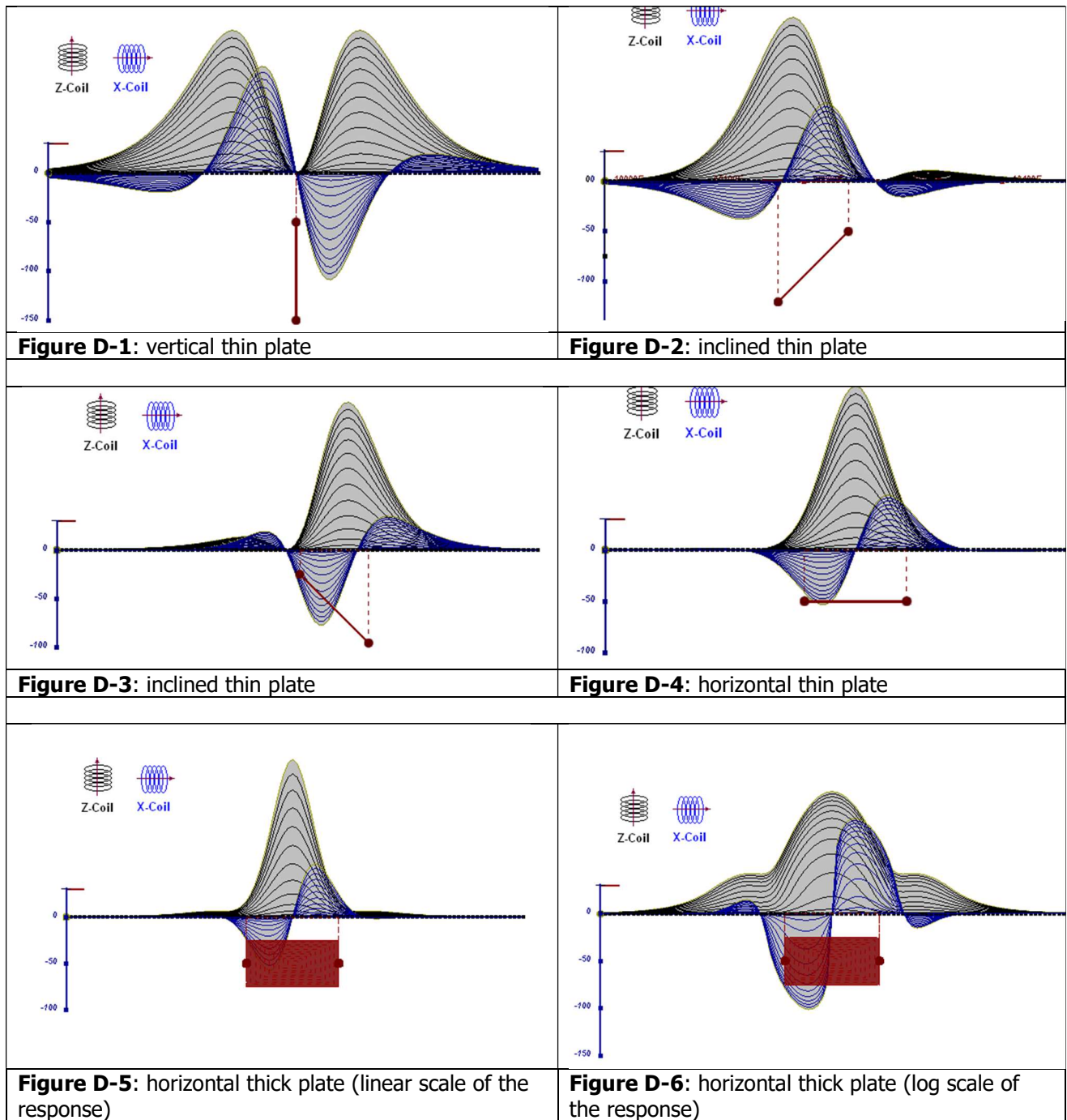
During turn-on and turn-off, a time varying field is produced (dB/dt) and an electro-motive force (emf) is created as a finite impulse response. A current ring around the transmitter loop moves outward and downward as time progresses. When conductive rocks and mineralization are encountered, a secondary field is created by mutual induction and measured by the receiver at the centre of the transmitter loop.

Efficient modeling of the results can be carried out on regularly shaped geometries, thus yielding close approximations to the parameters of the measured targets. The following is a description of a series of common models made for the purpose of promoting a general understanding of the measured results.

A set of models has been produced for the Geotech VTEM™ system dB/dT Z and X components (see models D1 to D15). The Maxwell™ modeling program (EMIT Technology Pty. Ltd. Midland, WA, AU) used to generate the following responses, assumes a resistive half-space. The reader is encouraged to review these models, so as to get a general understanding of the responses as they apply to survey results. While these models do not begin to cover all possibilities, they give a general perspective on the simple and most commonly encountered anomalies.

As the plate dips and departs from the vertical position, the peaks become asymmetrical.

As the dip increases, the aspect ratio (Min/Max) decreases and this aspect ratio can be used as an empirical guide to dip angles from near 90° to about 30°. The method is not sensitive enough where dips are less than about 30°.



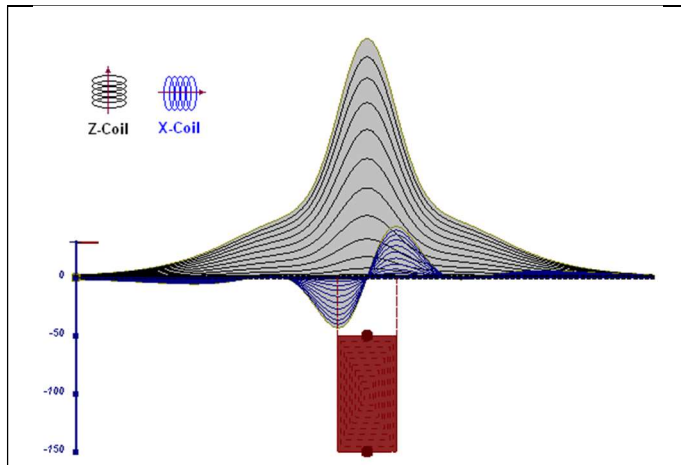


Figure D-7: vertical thick plate (linear scale of the response). 50 m depth

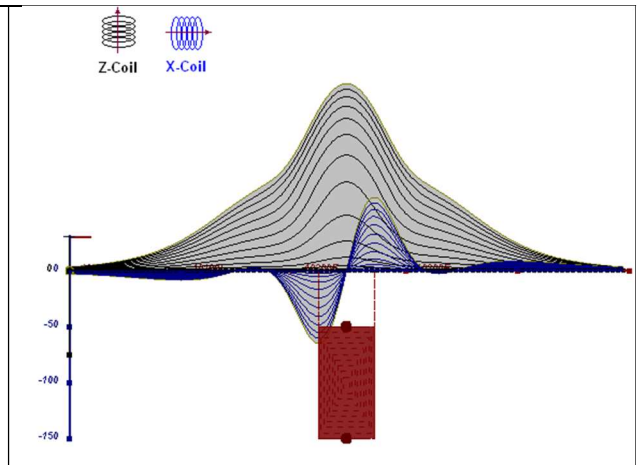


Figure D-8: vertical thick plate (log scale of the response). 50 m depth

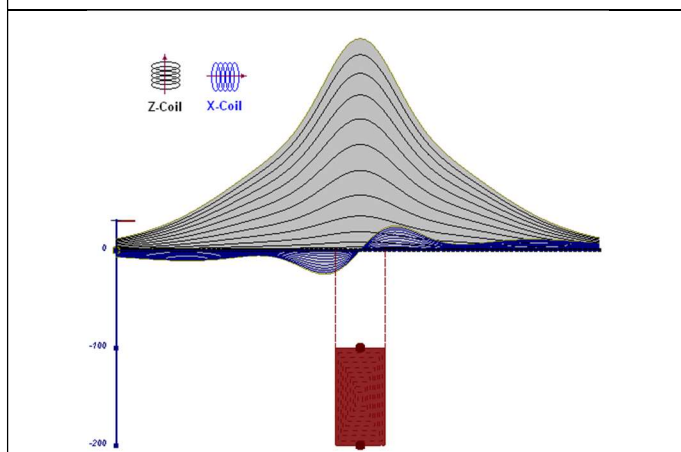


Figure D-9: vertical thick plate (linear scale of the response). 100 m depth

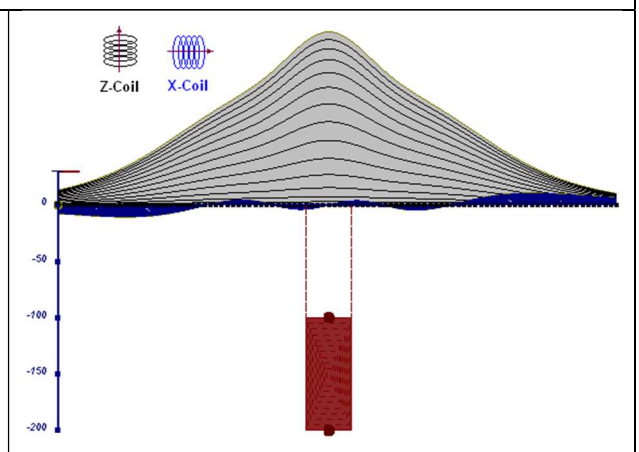


Figure D-10: vertical thick plate (linear scale of the response). Depth / horizontal thickness=2.5

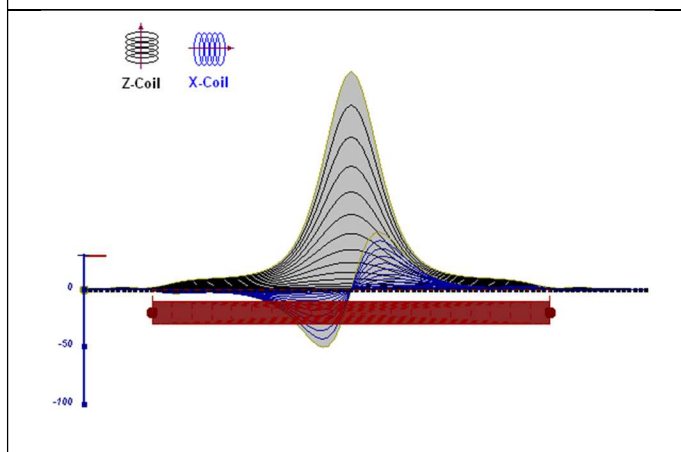


Figure D-11: horizontal thick plate (linear scale of the response)

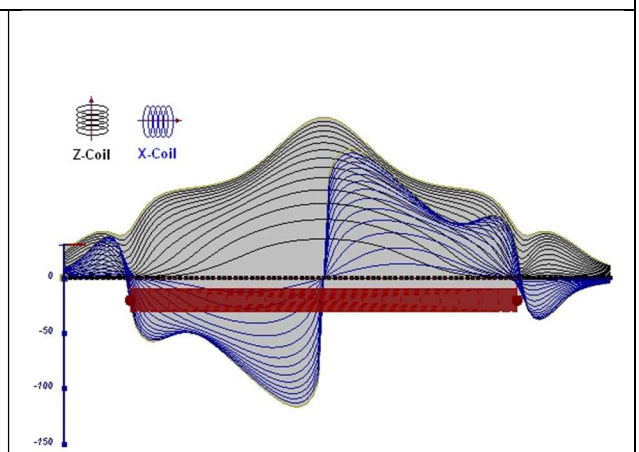


Figure D-12: horizontal thick plate (log scale of the response)

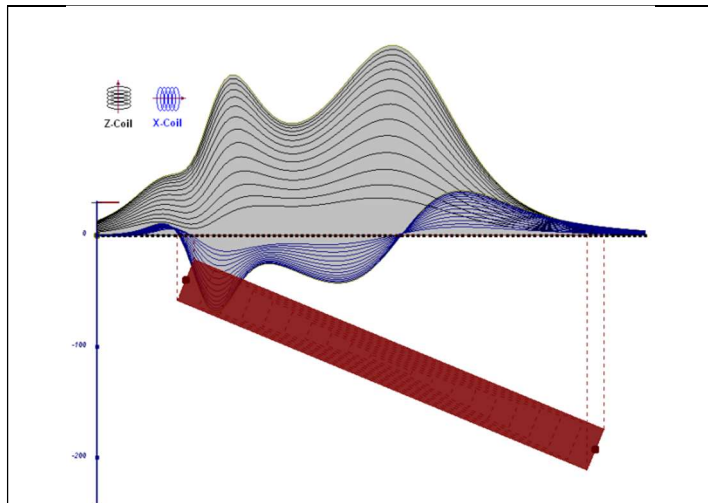


Figure D-13: inclined long thick plate

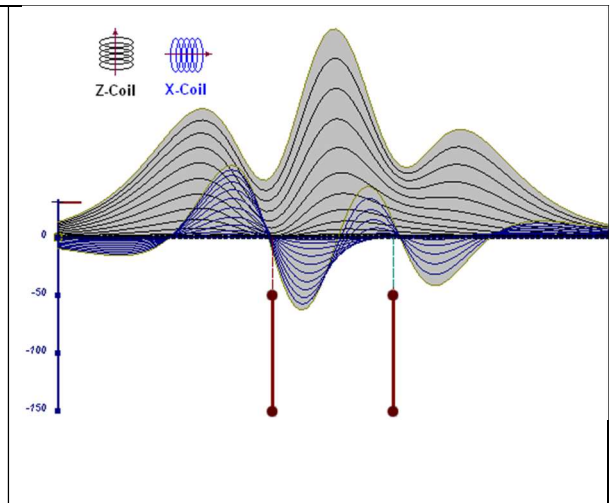


Figure D-14: two vertical thin plates

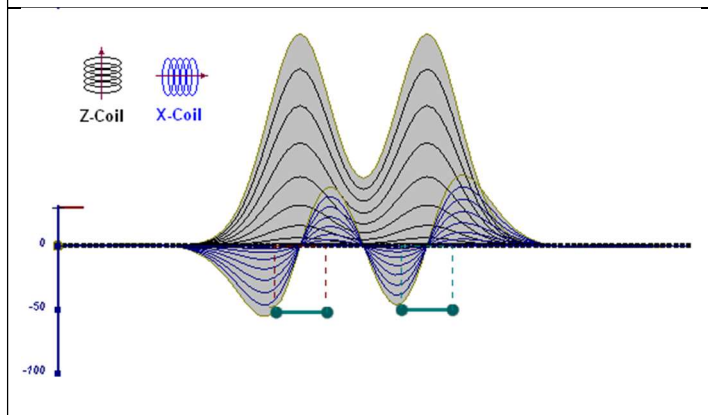


Figure D-15: two horizontal thin plates

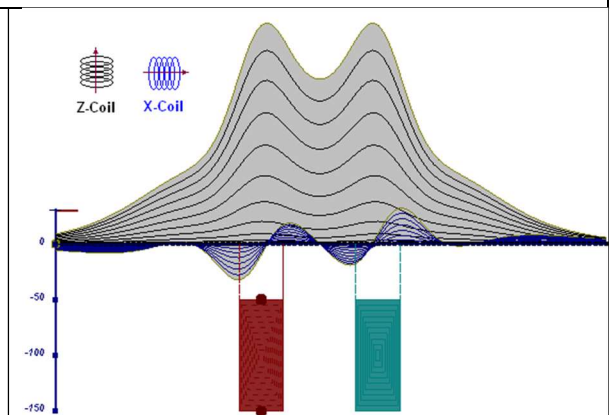


Figure D-16: two vertical thick plates

The same type of target but with different thickness, for example, creates different form of the response:

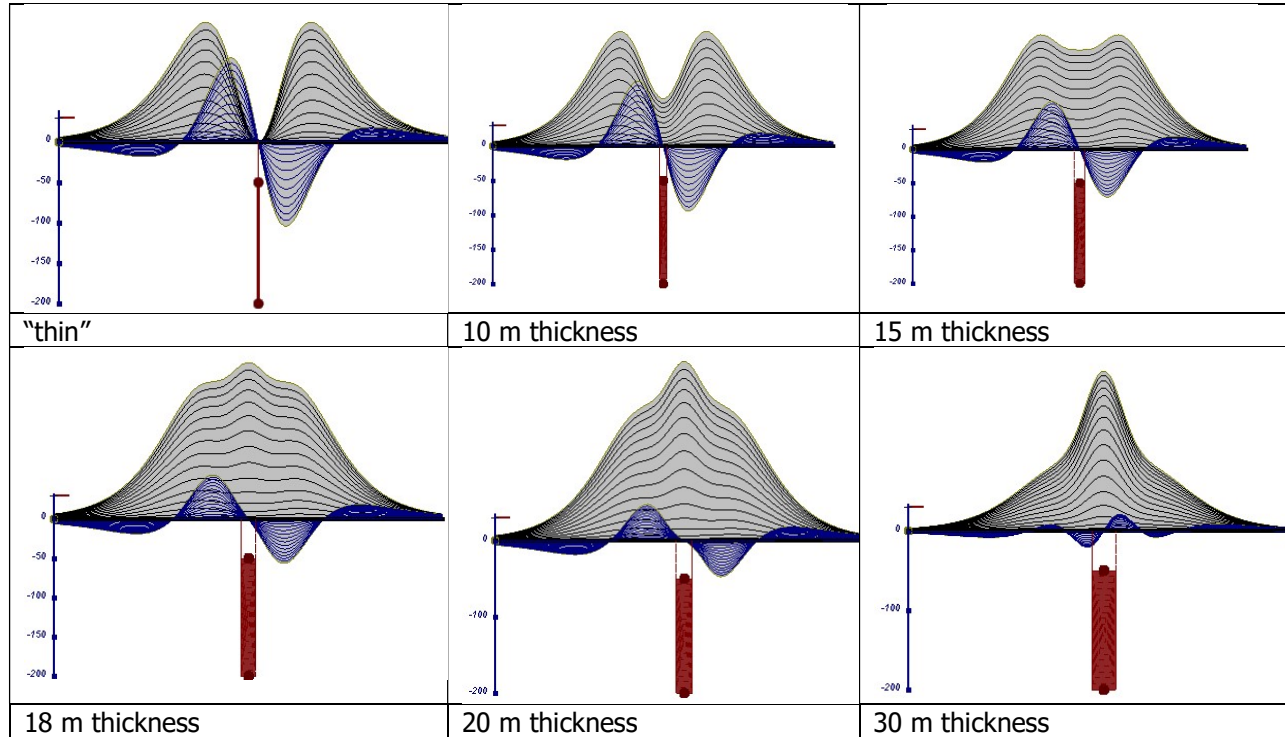


Figure D-17: Conductive vertical plate, depth 50 m, strike length 200 m, depth extends 150 m.

After Alexander Prikhodko
Geotech Ltd.

September 2010

APPENDIX E

EM TIME CONSTANT (TAU) ANALYSIS

Estimation of time constant parameter¹ in transient electromagnetic method is one of the steps toward the extraction of the information about conductances beneath the surface from TEM measurements.

The most reliable method to discriminate or rank conductors from overburden, background or one and other is by calculating the EM field decay time constant (TAU parameter), which directly depends on conductance despite their depth and accordingly amplitude of the response.

THEORY

As established in electromagnetic theory, the magnitude of the electro-motive force (emf) induced is proportional to the time rate of change of primary magnetic field at the conductor. This emf causes eddy currents to flow in the conductor with a characteristic transient decay, whose Time Constant (Tau) is a function of the conductance of the survey target or conductivity and geometry (including dimensions) of the target. The decaying currents generate a proportional secondary magnetic field, the time rate of change of which is measured by the receiver coil as induced voltage during the Off time.

The receiver coil output voltage (e_0) is proportional to the time rate of change of the secondary magnetic field and has the form,

$$e_0 \propto (1 / \tau) e^{-(t / \tau)}$$

Where,

$\tau = L/R$ is the characteristic time constant of the target (TAU)

R = resistance

L = inductance

From the expression, conductive targets that have small value of resistance and hence large value of τ yield signals with small initial amplitude that decays relatively slowly with progress of time. Conversely, signals from poorly conducting targets that have large resistance value and small τ , have high initial amplitude but decay rapidly with time¹ (Fig. E1).

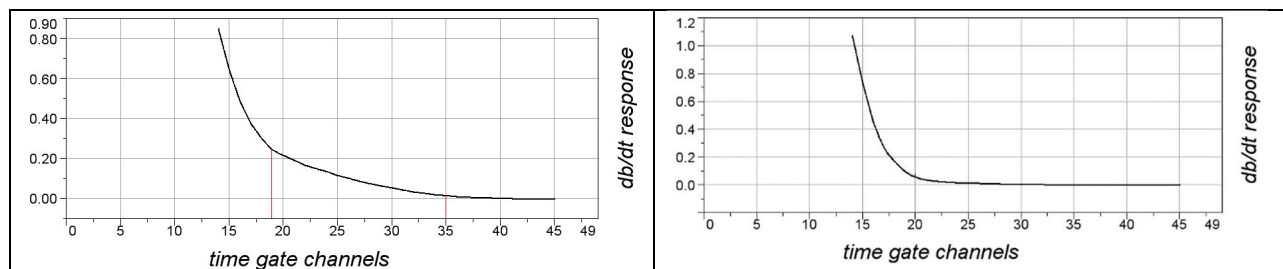


Figure E-1: Left – presence of good conductor, right – poor conductor.

¹ McNeill, JD, 1980, "Applications of Transient Electromagnetic Techniques", Technical Note TN-7 page 5, Geonics Limited, Mississauga, Ontario.

EM Time Constant (Tau) Calculation

The EM Time-Constant (TAU) is a general measure of the speed of decay of the electromagnetic response and indicates the presence of eddy currents in conductive sources as well as reflecting the “conductance quality” of a source. Although TAU can be calculated using either the measured dB/dt decay or the calculated B-field decay, dB/dt is commonly preferred due to better stability (S/N) relating to signal noise. Generally, TAU calculated on base of early time response reflects both near surface overburden and poor conductors whereas, in the late ranges of time, deep and more conductive sources, respectively. For example early time TAU distribution in an area that indicates conductive overburden is shown in Figure 2.

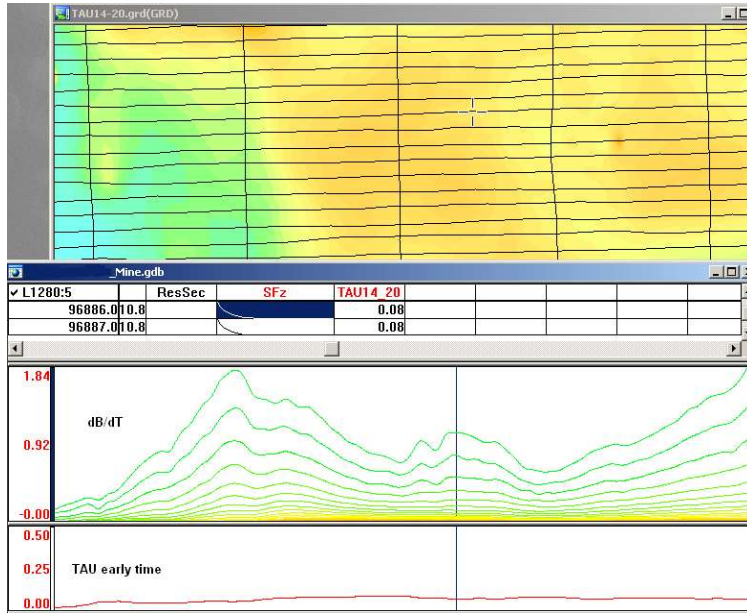


Figure E-2: Map of early time TAU. Area with overburden conductive layer and local sources.

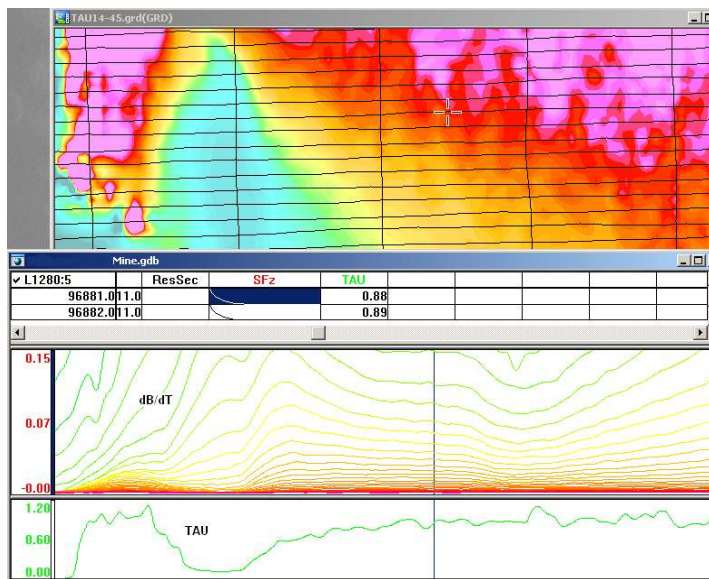


Figure E-3: Map of full time range TAU with EM anomaly due to deep highly conductive target.

There are many advantages of TAU maps:

- TAU depends only on one parameter (conductance) in contrast to response magnitude;
- TAU is integral parameter, which covers time range and all conductive zones and targets are displayed independently of their depth and conductivity on a single map.
- Very good differential resolution in complex conductive places with many sources with different conductivity.
- Signs of the presence of good conductive targets are amplified and emphasized independently of their depth and level of response accordingly.

In the example shown in Figure 4 and 5, three local targets are defined, each of them with a different depth of burial, as indicated on the resistivity depth image (RDI). All are very good conductors but the deeper target (number 2) has a relatively weak dB/dt signal yet also features the strongest total TAU (Figure 4). This example highlights the benefit of TAU analysis in terms of an additional target discrimination tool.

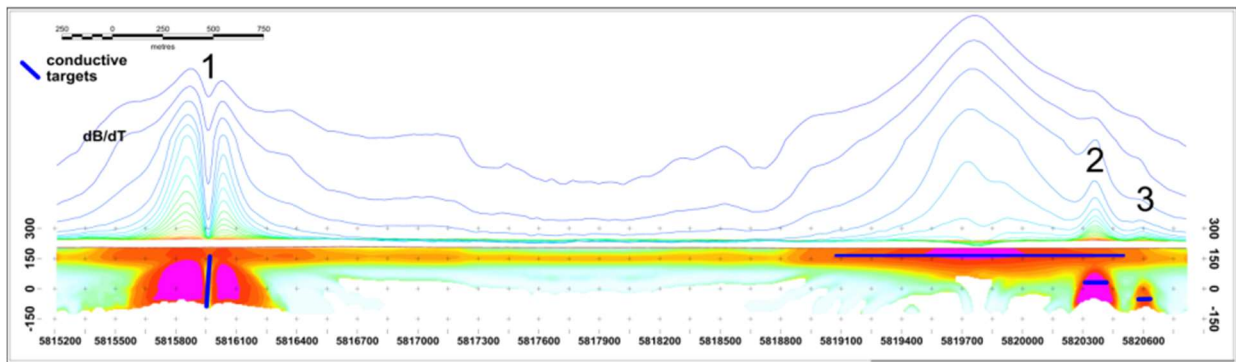


Figure E-4: dB/dt profile and RDI with different depths of targets.

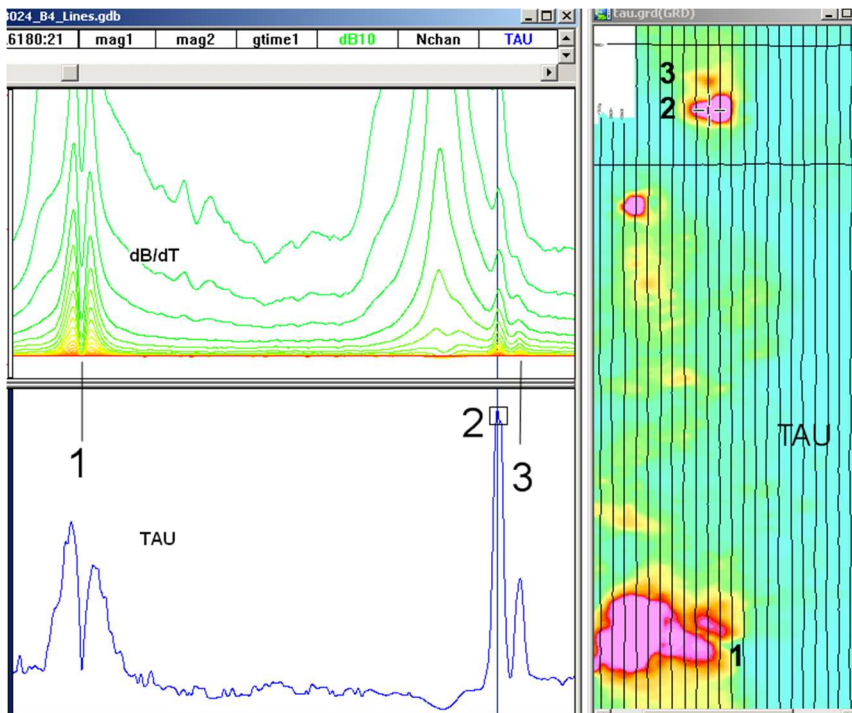


Figure E-5: Map of total TAU and dB/dt profile.

The EM Time Constants for dB/dt and B-field were calculated using the “sliding Tau” in-house program developed at Geotech2. The principle of the calculation is based on using of time window (4 time channels) which is sliding along the curve decay and looking for latest time channels which have a response above the level of noise and decay. The EM decays are obtained from all available decay channels, starting at the latest channel. Time constants are taken from a least square fit of a straight-line (log/linear space) over the last 4 gates above a pre-set signal threshold level (Figure F6). Threshold settings are pointed in the “label” property of TAU database channels. The sliding Tau method determines that, as the amplitudes increase, the time-constant is taken at progressively later times in the EM decay. Conversely, as the amplitudes decrease, Tau is taken at progressively earlier times in the decay. If the maximum signal amplitude falls below the threshold, or becomes negative for any of the 4 time gates, then Tau is not calculated and is assigned a value of “dummy” by default.

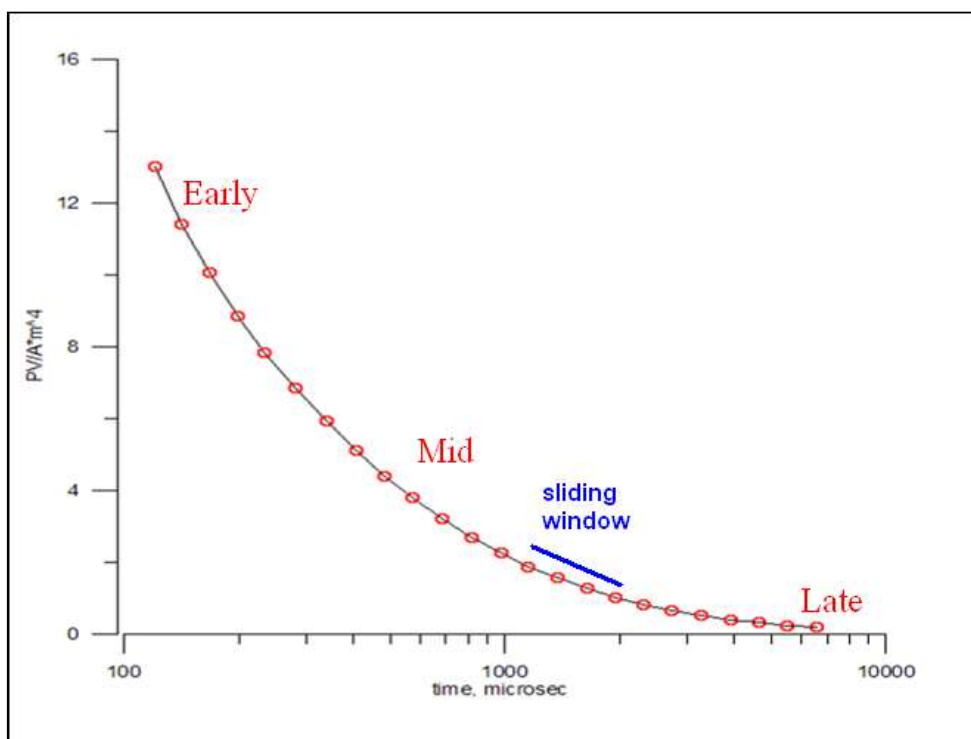


Figure E-6: Typical dB/dt decays of Vtem data

After Alexander Prikhodko
Geotech Ltd.

September 2010

² by A.Prihodko

APPENDIX F

TEM RESISTIVITY DEPTH IMAGING (RDI)

Resistivity depth imaging (RDI) is a technique used to rapidly convert EM profile decay data into an equivalent resistivity versus depth cross-section, by deconvolving the measured TEM data. The used RDI algorithm of Resistivity-Depth transformation is based on the scheme of the apparent resistivity transform of Maxwell A. Meju (1998)¹ and TEM response from a conductive half-space. The program is developed by Alexander Prikhodko and is depth calibrated based on forward plate modeling for VTEM system configuration (Fig. 1-10).

RDIs provide reasonable indications of conductor relative depth and vertical extent, as well as accurate 1D layered-earth apparent conductivity/resistivity structure across VTEM flight lines. Approximate depth of investigation of a TEM system, image of secondary field distribution in half-space, effective resistivity, initial geometry and position of conductive targets is the information obtained on the basis of the RDIs.

Maxwell forward modeling with RDI sections from the synthetic responses (VTEM system).

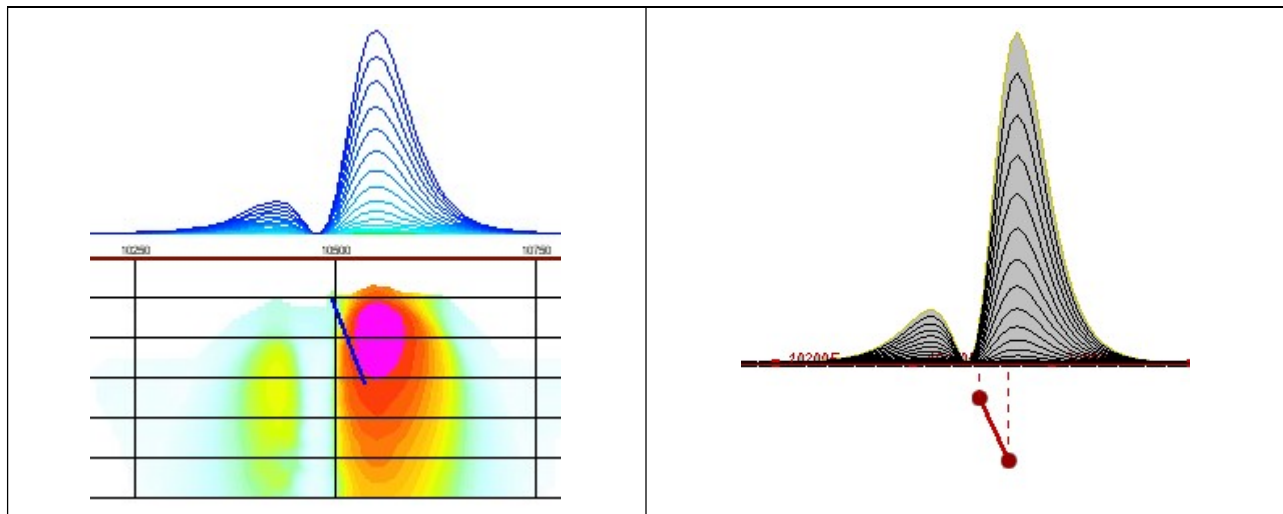


Figure F-1: Maxwell plate model and RDI from the calculated response for a conductive "thin" plate (depth 50 m, dip 65 degree, depth extend 100 m).

¹ Maxwell A. Meju, 1998, Short Note: A simple method of transient electromagnetic data analysis, *Geophysics*, **63**, 405–410.

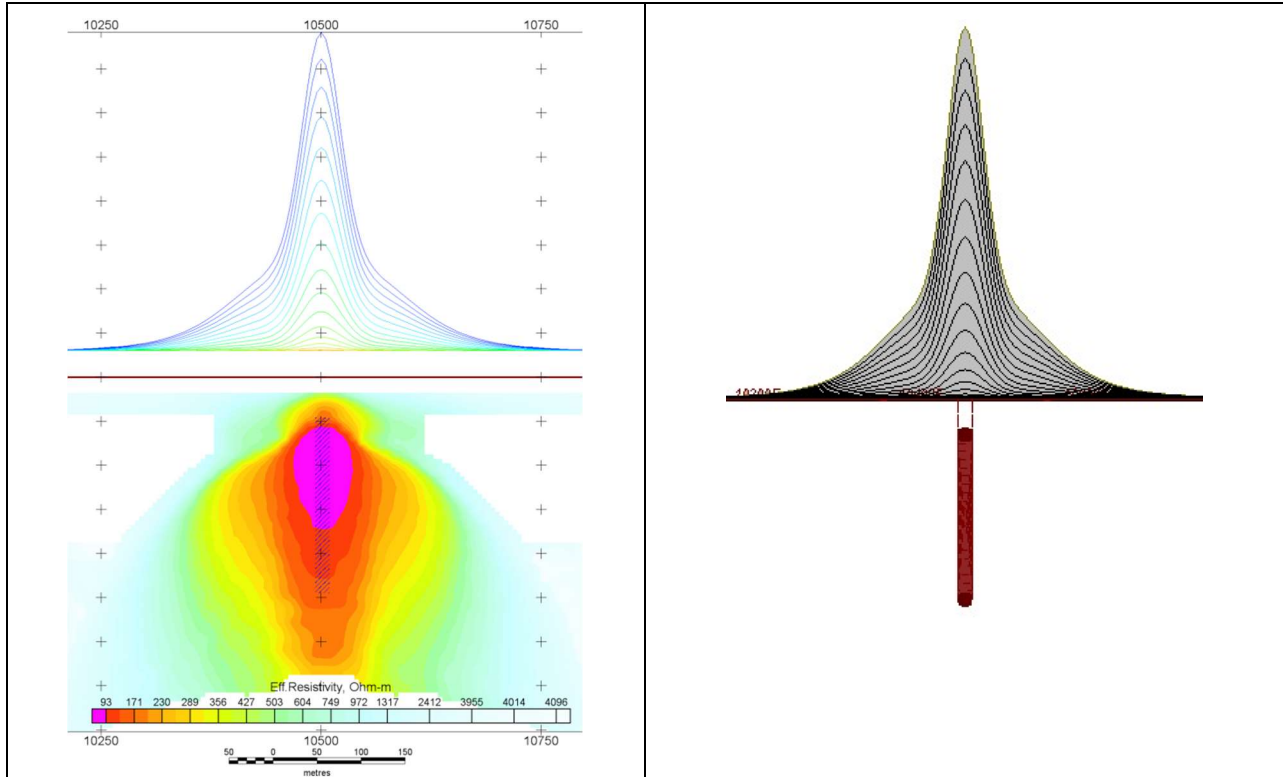


Figure F-2: Maxwell plate model and RDI from the calculated response for "thick" plate 18 m thickness, depth 50 m, depth extend 200 m).

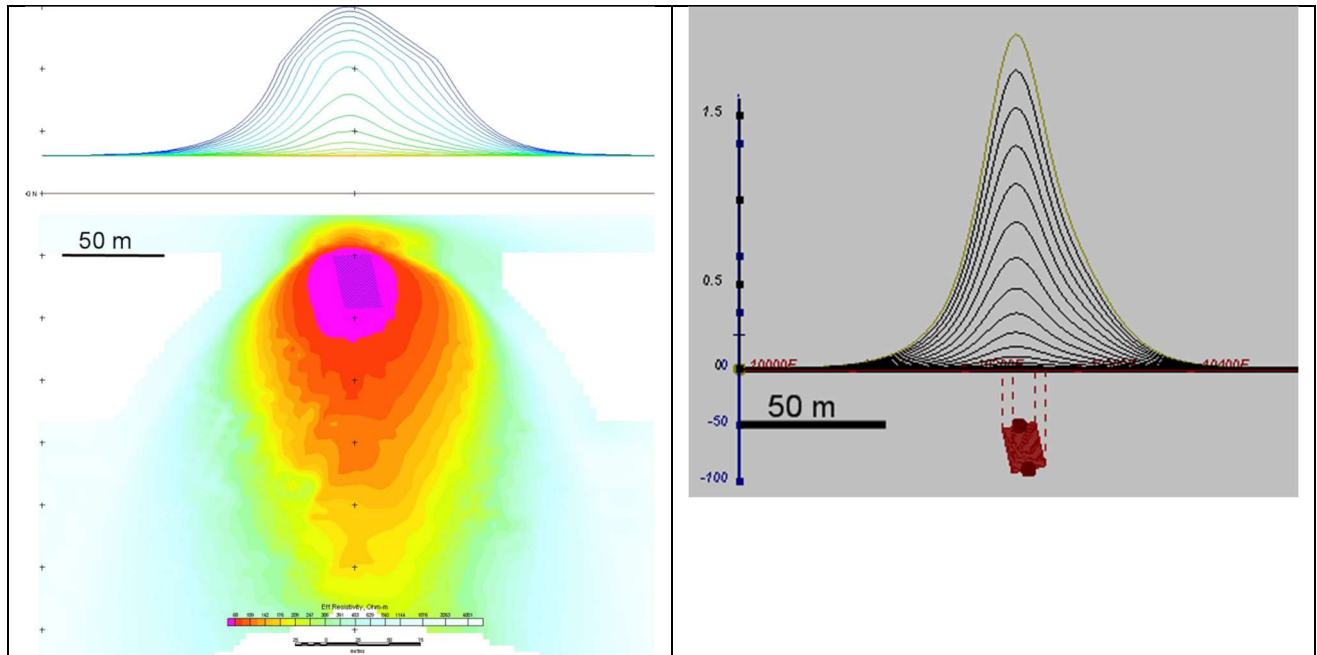


Figure F-3: Maxwell plate model and RDI from the calculated response for bulk ("thick") 100 m length, 40 m depth extend, 30 m thickness

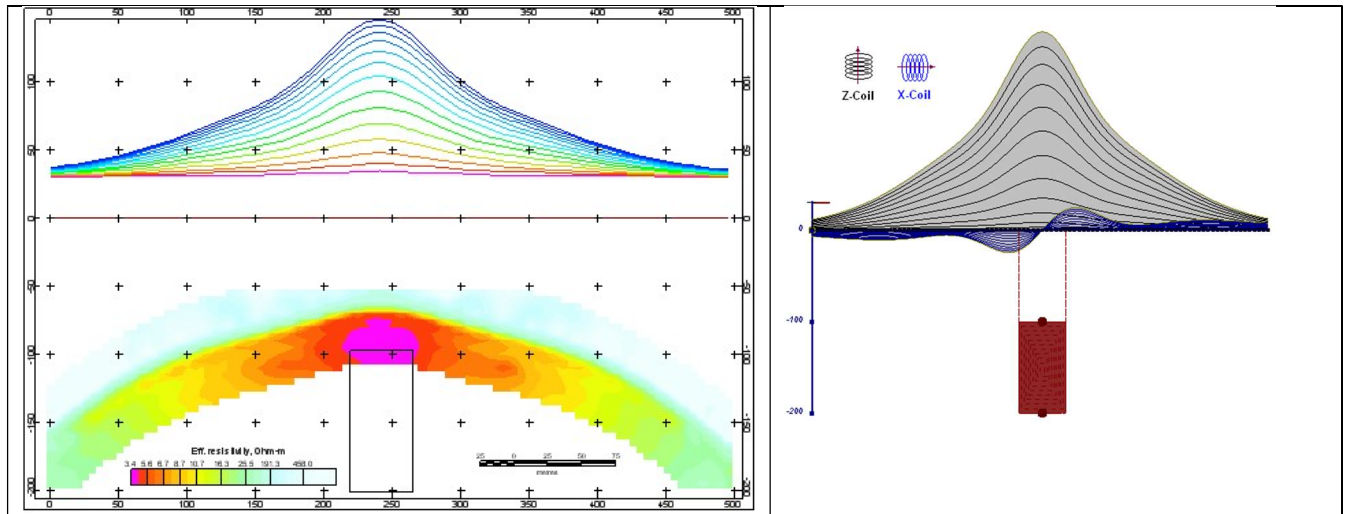


Figure F-4: Maxwell plate model and RDI from the calculated response for "thick" vertical target (depth 100 m, depth extend 100 m). 19-44 chan.

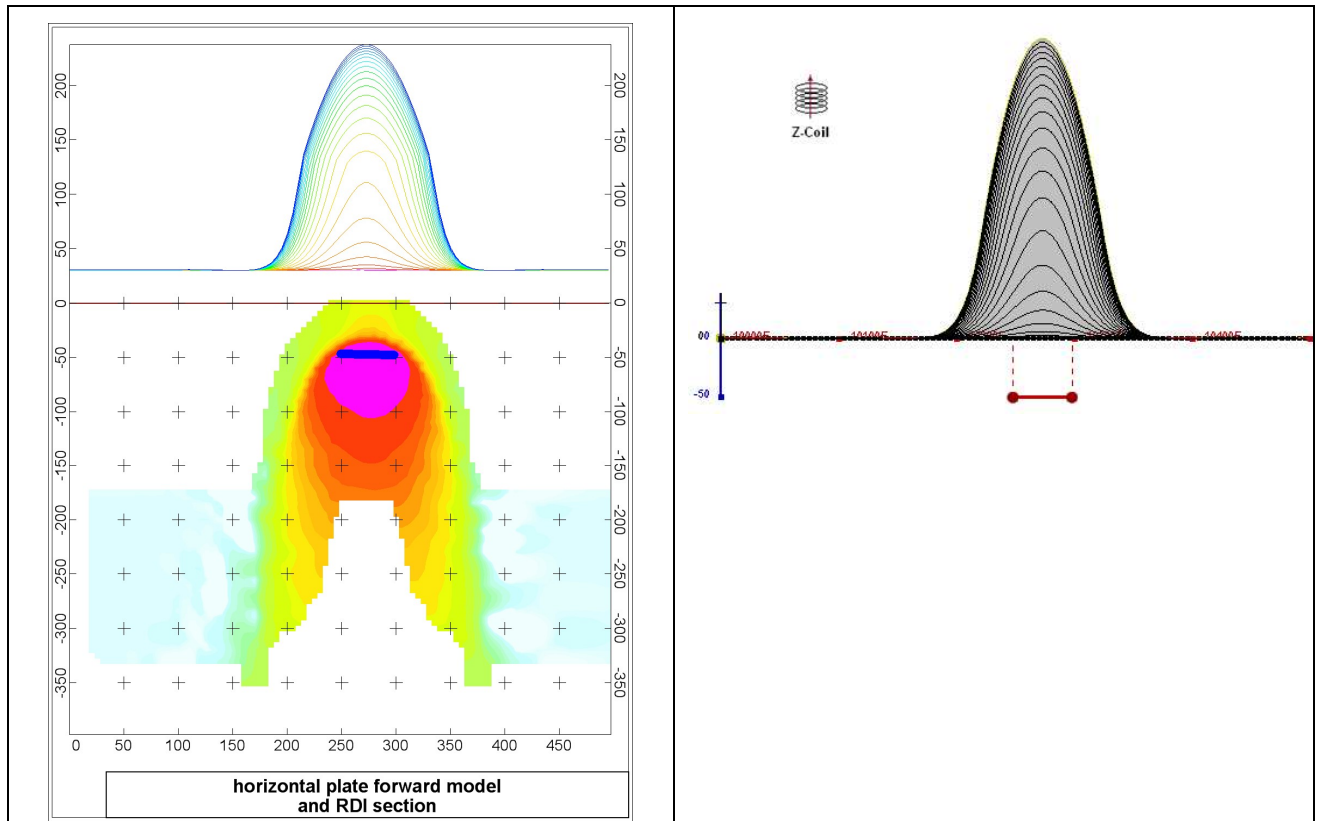


Figure F-5: Maxwell plate model and RDI from the calculated response for horizontal thin plate (depth 50 m, dim 50x100 m). 15-44 chan.

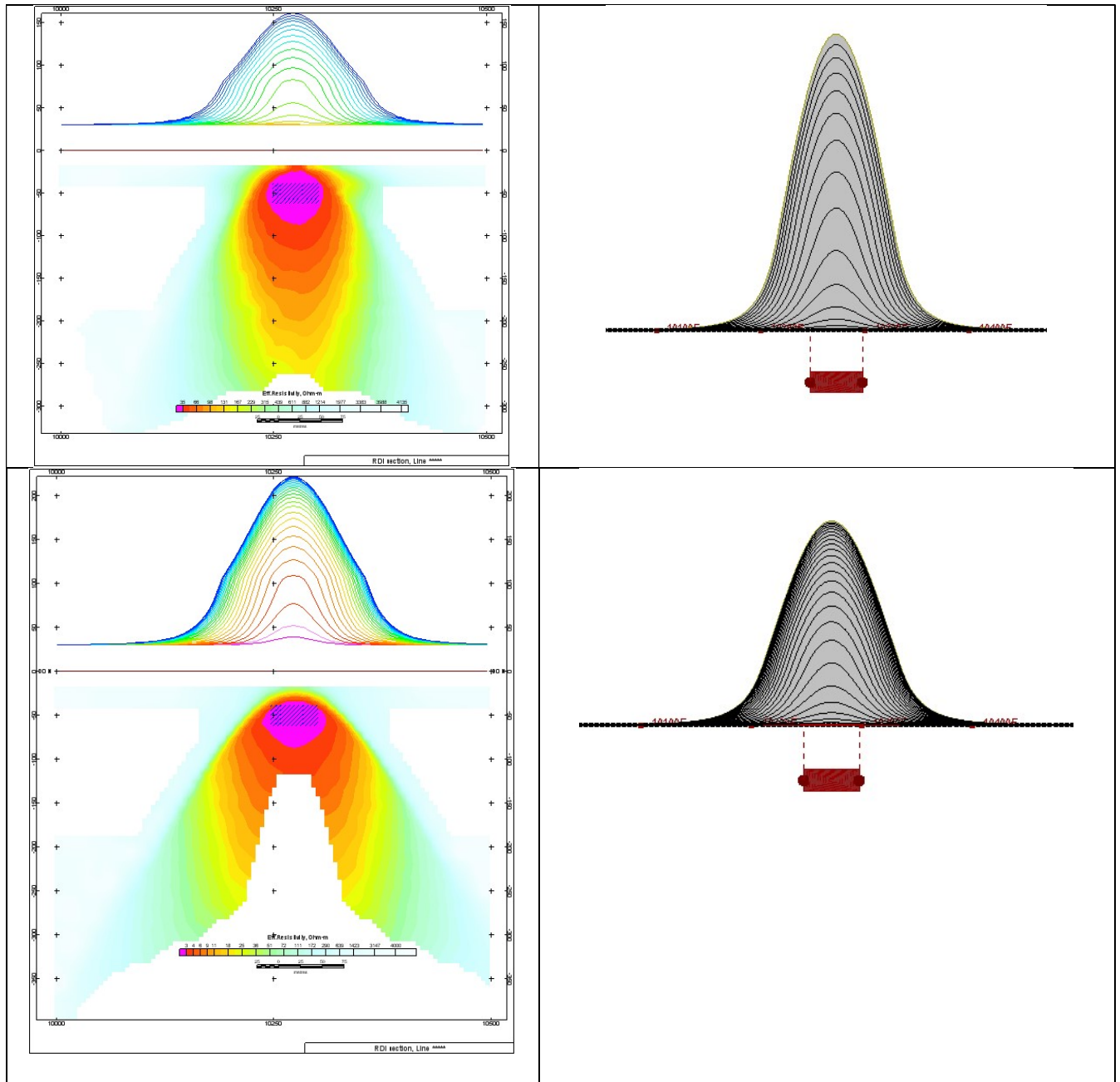


Figure F-6: Maxwell plate model and RDI from the calculated response for horizontal thick (20m) plate – less conductive (on the top), more conductive (below).

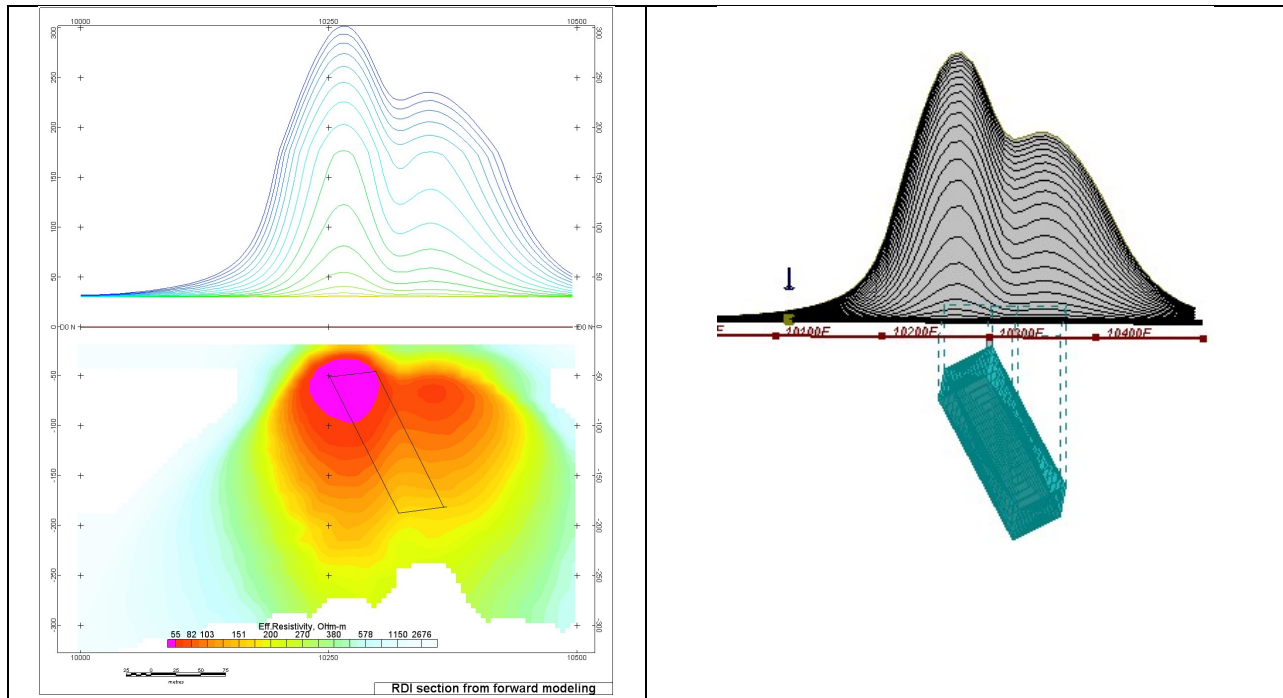


Figure F-7: Maxwell plate model and RDI from the calculated response for inclined thick (50m) plate. Depth extends 150 m, depth to the target 50 m.

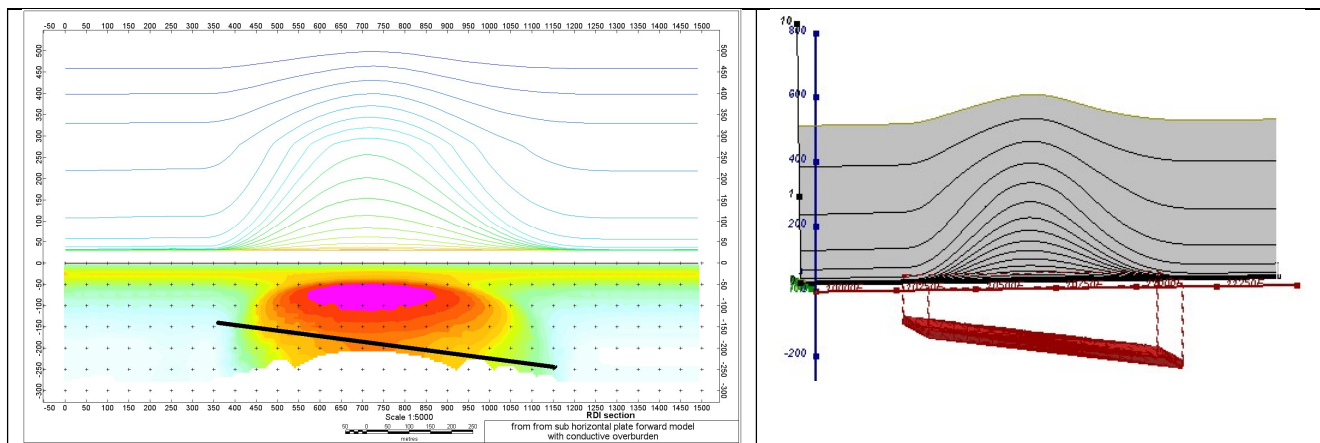


Figure F-8: Maxwell plate model and RDI from the calculated response for the long, wide and deep subhorizontal plate (depth 140 m, dim 25x500x800 m) with conductive overburden.

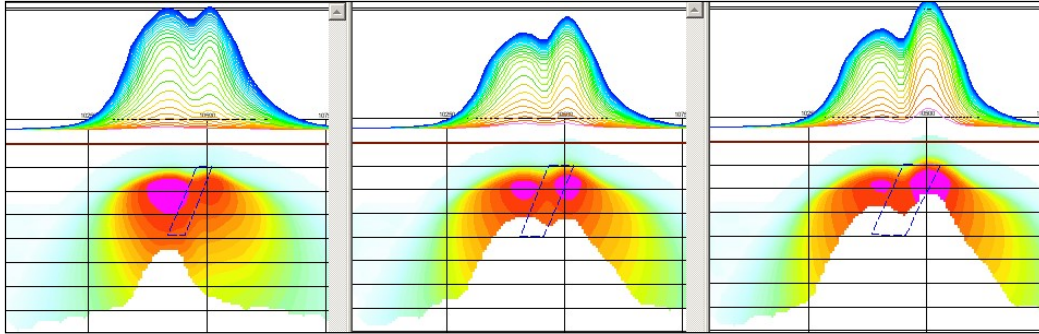


Figure F-9: Maxwell plate models and RDIs from the calculated response for "thick" dipping plates (35, 50, 75 m thickness), depth 50 m, conductivity 2.5 S/m.

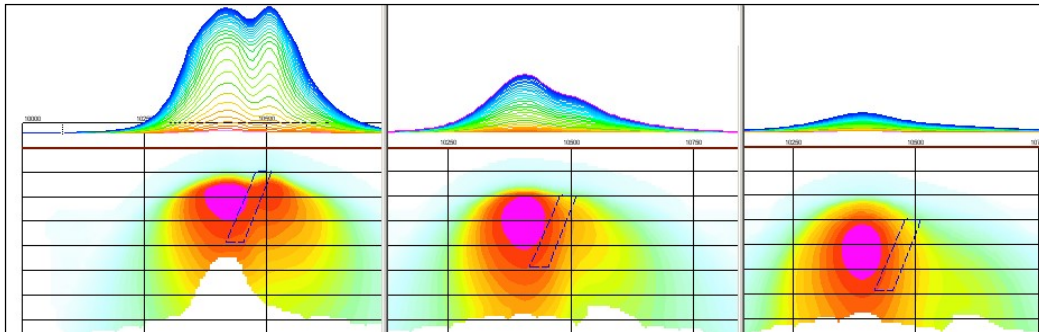


Figure F-10: Maxwell plate models and RDIs from the calculated response for "thick" (35 m thickness) dipping plate on different depth (50, 100, 150 m), conductivity 2.5 S/m.

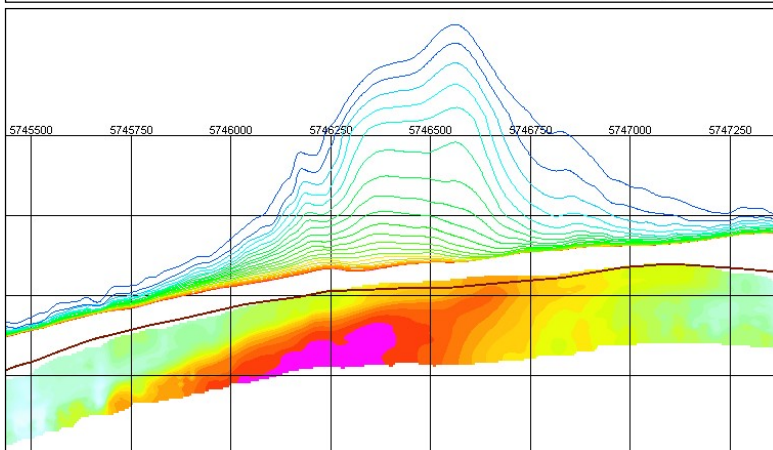
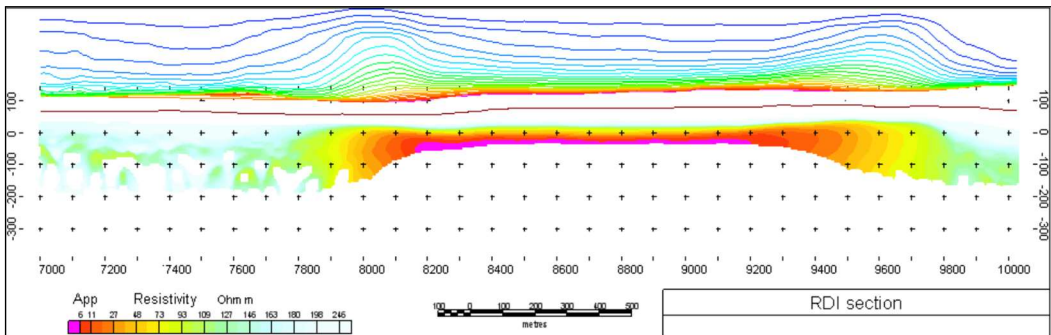
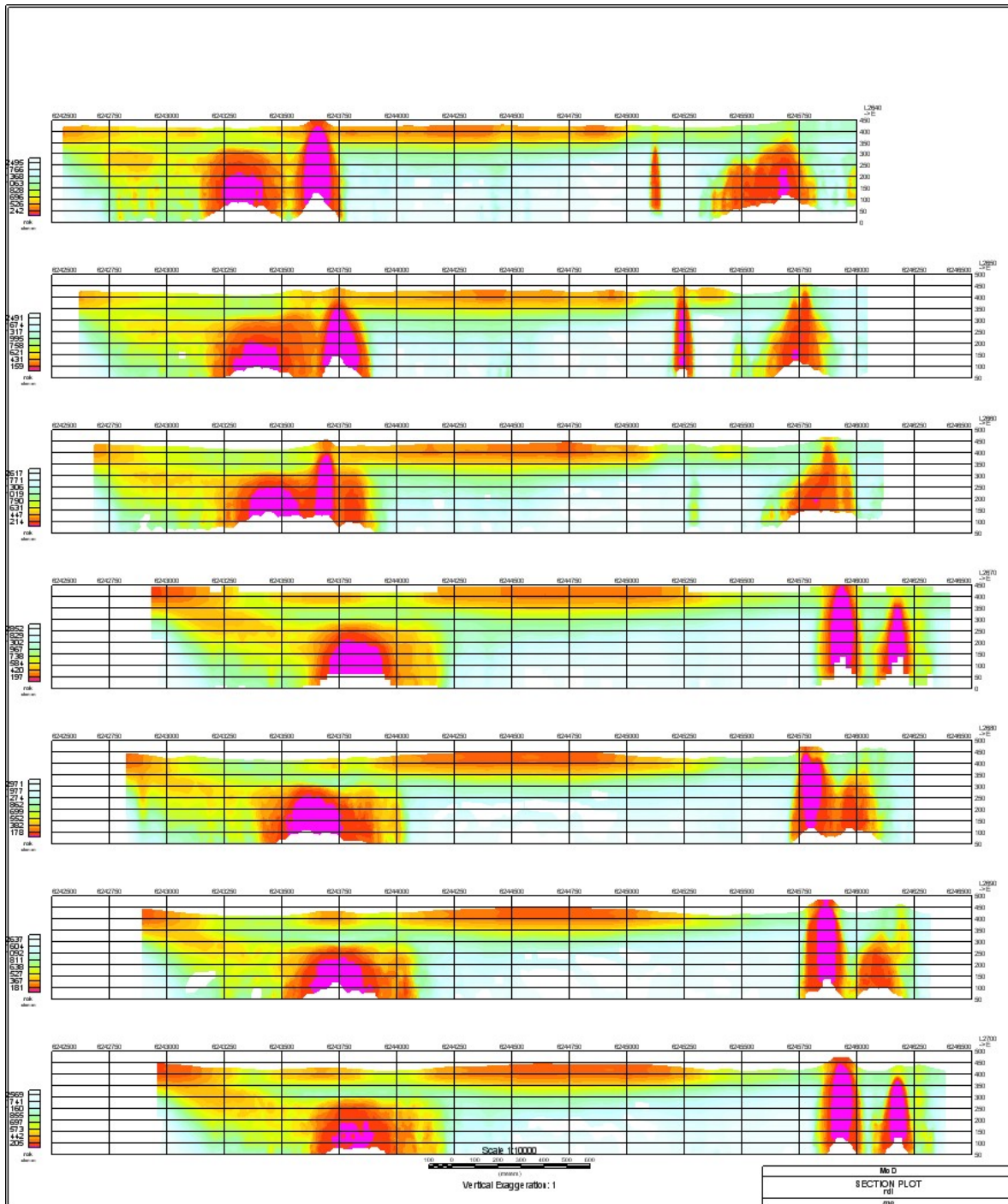


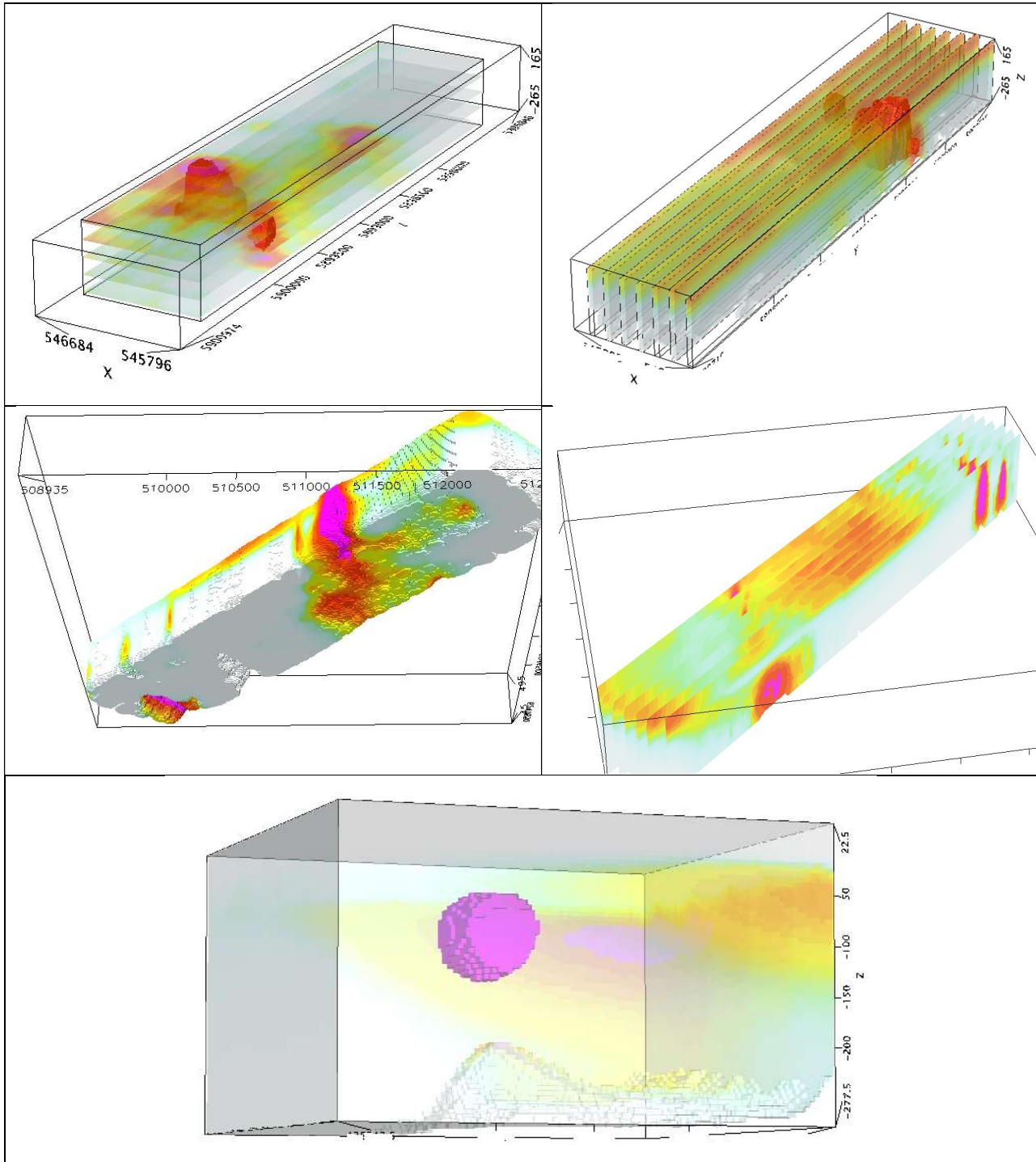
Figure F-11: RDI section for the real horizontal and slightly dipping conductive layers

FORMS OF RDI PRESENTATION

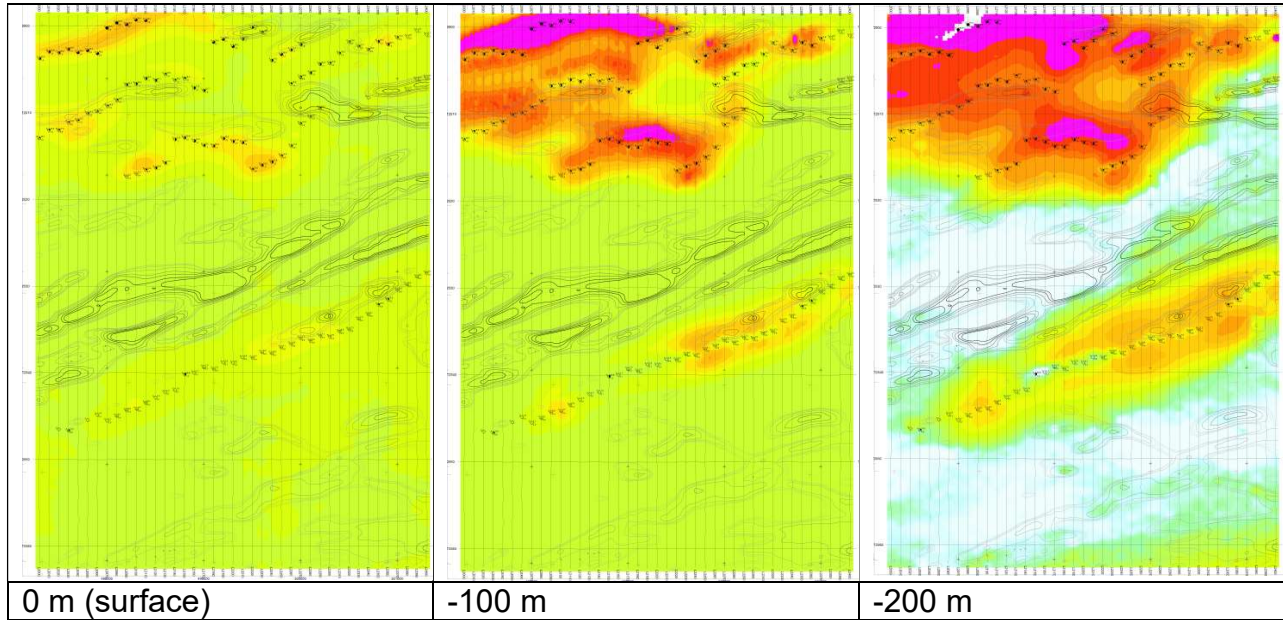
PRESENTATION OF SERIES OF LINES



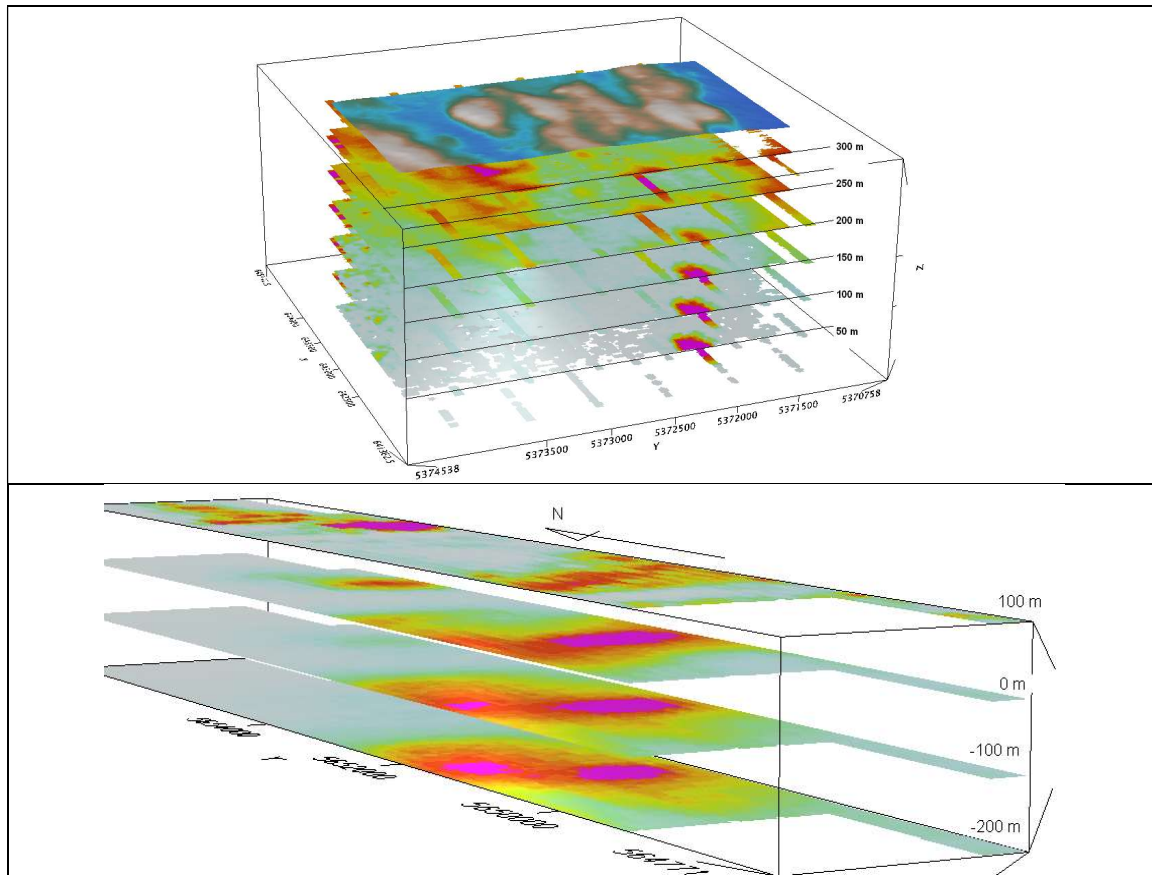
3D PRESENTATION OF RDIS



APPARENT RESISTIVITY DEPTH SLICES PLANS:

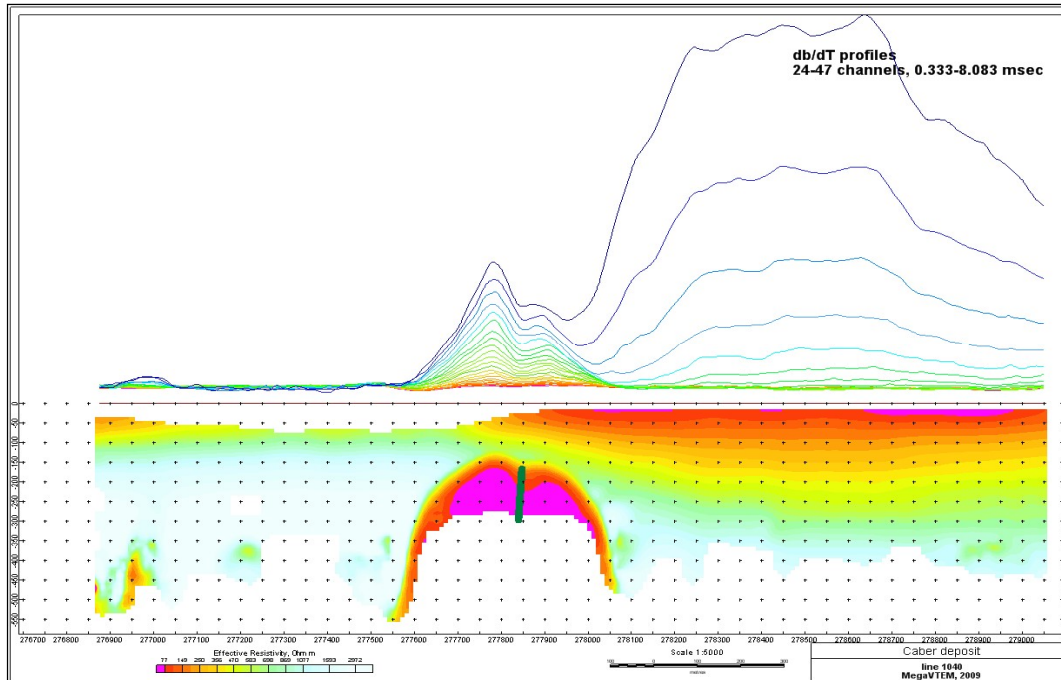


3D VIEWS OF APPARENT RESISTIVITY DEPTH SLICES:

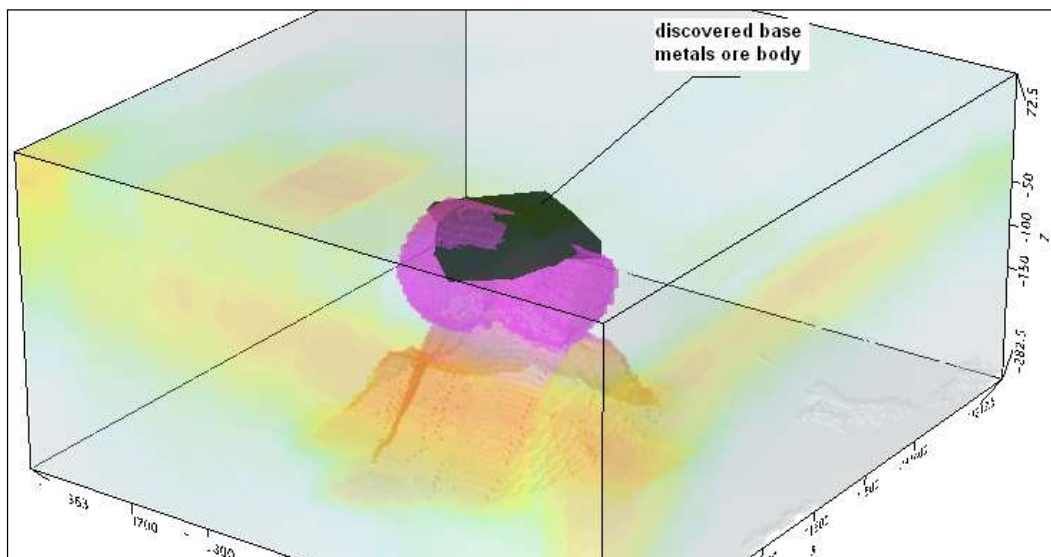


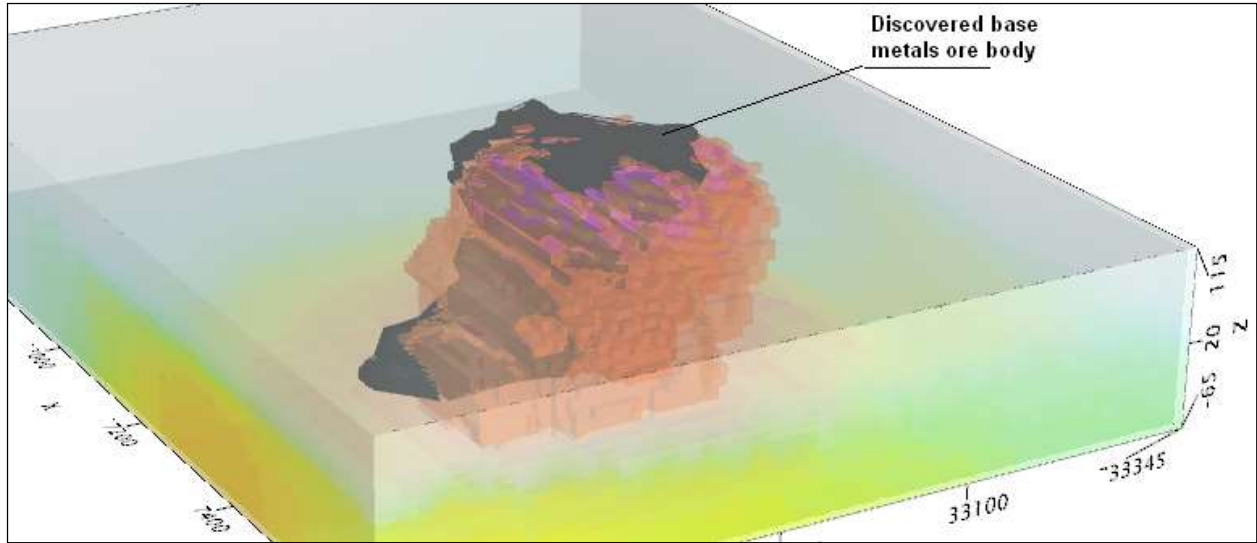
REAL BASE METAL TARGETS IN COMPARISON WITH RDIS:

RDI section of the line over Caber deposit ("thin" subvertical plate target and conductive overburden).



3D RDI VOXELS WITH BASE METALS ORE BODIES (MIDDLE EAST):





After Alexander Prikhodko
Geotech Ltd.
April 2011

APPENDIX G

RESISTIVITY DEPTH IMAGES (RDI)

Please see RDI Folder on DVD for the PDF's